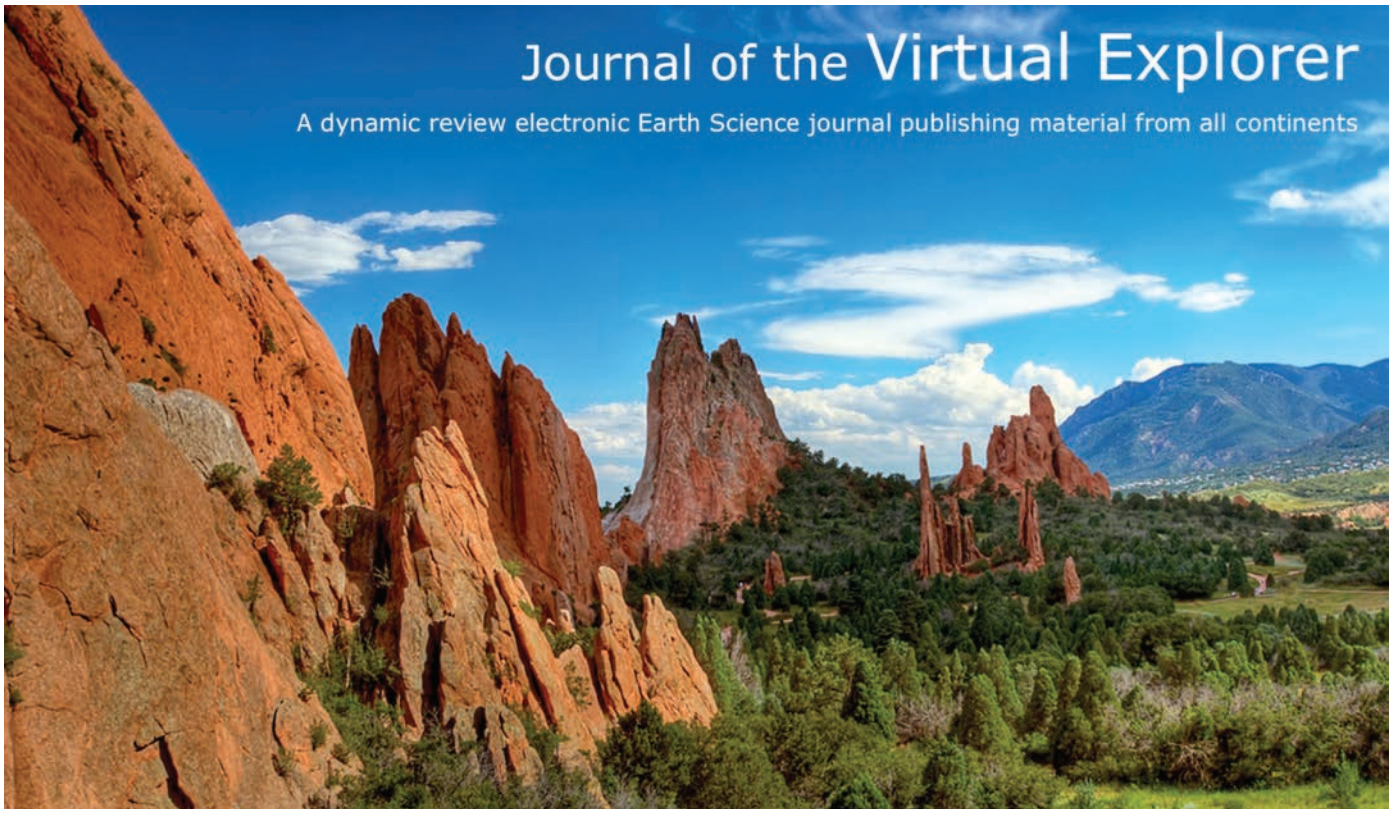

The Higher Himalayan Crystallines, Alaknanda – Dhauli Ganga Valleys, Garhwal Himalaya, India

Jain A. K., Shreshtha M., Seth P., Kanyal L., Carosi R., Montomoli C., Iaccarino S., Mukherjee P. K.

Journal of the VIRTUAL EXPLORER, Electonic Edition, ISSN 1441-8142, volume 47, Paper 8, In: (Eds) Chiara Montomoli, Rodolfo Carosi, Rick Law, Sandeep Singh, Santa Man Rai, Geological field trips in the Himalaya, Karakoram and Tibet, 2014

Journal of the VIRTUAL EXPLORER

A dynamic review electronic Earth Science journal publishing material from all continents

The Higher Himalayan Crystallines, Alaknanda – Dhauli Ganga Valleys, Garhwal Himalaya, India

Jain A. K.[1], Shreshtha M.[2], Seth P.[2], Kanyal L.[2], Carosi R. [3], Montomoli C.[4], Iaccarino S. [4], Mukherjee P. K.[5]

[1]CSIR-Central Building research Institute, Roorkee-247667, India.
[2]Department of Earth Sciences, Indian Institute of Technology, Roorkee-247667, India.
[3]Department of Earth Sciences, University of Torino, via Valperga Caluso 35, I-10125, Torino, Italy.
[4]Department of Earth Sciences, University of Pisa, via S. Maria 53, I-56126, Pisa, Italy
[5]Wadia Institute of Himalayan Geology, Dehra Dun-248001, India.

GUIDE INFO

Keywords
Higher Himalayan Crystallines (HHC)
Deformation
Tectonic evolution
Migmatite and leucogranite emplacement

Citation
Jain, A.K., Shreshtha, M., Seth, P., Kanyal, L., Carosi, R., Montomoli, C., Iaccarino, S., and Mukherjee, P.K. 2014. The Higher Himalayan Crystallines, Alaknanda – Dhauli Ganga Valleys, Garhwal Himalaya, India. In: (Eds.) Chiara Montomoli, Rodolfo Carosi, Rick Law, Sandeep Singh, and Santa Man Rai, Geological field trips in the Himalaya, Karakoram and Tibet, Journal of the Virtual Explorer, Electronic Edition, ISSN 1441-8142, volume 47, paper 8, DOI: 10.3809/jvirtex.2014.00349

Correspondence to:
himalfes@gmail.com

IN THIS GUIDE

In central parts of Uttarakhand, more than 20 km thick homoclinal NE-dipping Higher Himalayan Crystalline (HHC) belt is almost continuously exposed between Helang and Malari along the Dhauli Ganga Valley, and is thrust over the Lesser Himalaya along the Main Central Thrust (MCT). This road dip-section traverse provides an excellent opportunity to investigate the (i) ambiguity regarding the position and definition of the MCT in terms of the Munsiari Thrust (the MCT–I), and the Vaikrita Thrust (the MCT–II), (ii) position of the South Tibetan Detachment System (STDS), (iii) deformation of the HHC, based on detailed shear sense analysis exhibiting top-to-south and top-to-north shear indicators, (iv) structural control on melt accumulation of the Himalayan migmatites and leucogranite, (v) Himalayan inverted metamorphism, and (vi) assessment of channel flow or other models for the exhumation of deep-seated crustal rocks.

Based on lithologies and metamorphic grade from the lower to higher structural levels northeastwards, the HHC is divisible into two main groups above the Munsiari Thrust (MCT). In the lower parts, the Munsiari Group of low to medium grade contains a highly mylonitized package of garnet mica schist/gneiss, quartzite, amphibolite and biotite-rich phyllonite, mylonitic gneiss and augen gneiss. Delineated by the Vaikrita Thrust (VT) the overlying Vaikrita Group is comprised of the Joshimath Formation (garnet-biotite-muscovite schist/psammitic gneiss), the Suraithota Formation (kyanite-garnet-biotite schist/psammitic gneiss and amphibolite), and the Bhapkund Formation (sillimanite/fibrolite-kyanite-garnet-biotite psammitic gneiss/schist with pervasive migmatite, concordant to discordant pegmatite veins, and small tourmaline-rich leucogranite lenses/dykes and the Malari leucogranite). The Vaikrita Group is typically characterized by inverted metamorphism, where sillimanite–K-feldspar gneiss and migmatite in uppermost parts of the Bhapkund Formation was metamorphosed under upper amphibolite facies at > 650 °C. The Bhapkund Formation constitutes the footwall of the STDS, which separates it from the very low biotite-grade to unmetamorphosed quartzite and slates/phyllite of the Martoli Formation of the basal Tethyan Sedimentary zone under peak metamorphic conditions of 450 ± 50 °C.

Many shear indicators can be recognized between Helang and Malari. Asymmetry of structures like S-C and S-C' fabric, asymmetric boudins, mantled porphyroclasts, folds etc. revealed top-to-the-north downward or northeast shear sense near the STDS and top-to-the-south upwards or southwest in large parts of the HHC and provide invaluable evidences for the direction of tectonic transport.

The Helang-Joshimath-Malari traverse along the Alaknanda – Dhauli Ganga Valleys provides excellent cross-section through the HHC and can be thoroughly investigated within 7 days, starting from Helang, located about 500 km from the Delhi Airport. A road/train connection from Delhi brings you to Holy city of Haridwar, located in the proximity of the Main Frontal Thrust (MFT). Travelling further north to Joshimath (275 Km from Haridwar) and camping for two days here, one can see the section between Helang – Joshimath – Tapovan (15 km) upstream in investigating the Munsiari Thrust, Vaikrita Thrust and lower package of the HHC, i.e. the Munsiari Group rocks. One locates the MCT about 12 km downstream from Joshimath near Helang. As the whole section is about 65 km long, it would be advisable to shift the camp to Malari to investigate the upper parts of the HHC from this picturesque village. The STDS is best exposed around this village along with a fully-developed migmatite sequence (the Bhapkund Formation), inverted metamorphism and shear indicators showing both top-to-SW upwards and top-to-NE downwards shear senses. One can traverse up to Niti village to look into the Tethyan Zone (TZ) before returning to Joshimath. After completing the whole section, various tectonic models can be critically assessed for the evolution of the Himalayan metamorphic belt.

INTRODUCTION

The India-Asia convergence resulted in intense crustal shortening in the Himalaya since Paleocene (Searle et al., 1987; Zhu et al., 2005; Yin, 2006, Jain, 2014). It has mobilized the northern edge of the Indian Plate during the Cenozoic into a vast metamorphic belt including the metamorphic core of the belt, represented by the Higher Himalayan Crystallines (HHC). This belt is thrust southwards on to the sedimentary belt of the Proterozoic Lesser Himalayan Sequence (LHS) along the Main Central Thrust (MCT) (Heim and Gansser 1939; Le Fort 1975; Gansser, 1964; Hodges, 2000; Jain et al., 2002; Yin, 2006). The metamorphic core of the Himalayan Orogen in the Eastern Garhwal region of the NW India consists of nearly 20 km thick homoclinal sequence of amphibolite-granulite facies HHC (Fig. 1), and is covered by the late Precambrian to Eocene Tethyan zone (TZ). The latter is bounded by the Indus-Tsangpo Suture zone (ITSZ) along its northern margin and the South Tibetan Detachment System (STDS) in the south (Burg et al., 1984; Burchfiel et al., 1992; Hodges, 2000).

The MCT with its zones of inverted metamorphic isograds from sillimanite grade down to biotite grade is one of the largest ductile shear zones known from any collision-related mountain belt. The MCT crops out along 2200 km length of the Himalaya from western Zanskar to Bhutan and Arunachal Pradesh (Searle et al., 2008; Jessup et al., 2008; Yin, 2006; Kellet et al., 2010). It dips north and places high-grade metamorphic rocks of the HHC south over unmetamorphosed or slightly metamorphosed rocks of the LHS all through its length. The HHC contains the most metamorphic rocks of the Himalayan orogen south of the Indus-Tsangpo Suture zone, and therefore is a key to understand the metamorphic evolution and degree of exhumation within the orogen (Kohn et al., 2005). Exhumation of the HHC also in the Garhwal region is associated with southwestward directed thrust sense of shear along the MCT, focused erosion at the denudational front, and northeastward directed normal-sense shear along the STDS. As a consequence of this convergence, one of the most spectacular result was the melting of various rock types of the HHC and generation of migmatite and leucogranite, which have been recently modeled as midcontinental crustal channel flow extruding into the southward translating HHC (Beaumont et al., 2001; Godin et al., 2006; Grujic et al., 2002; Jamieson et al., 2004; Searle et al., 2006, 2010).

The STDS juxtaposes the unmetamorphosed TZ down to the northeast over the high-grade metamorphic rocks of the HHC (Caby et al., 1983; Virdi, 1986; Patel et al., 1993; Gururajan and Choudhuri, 1999). The South Tibet Detachment System (STDS) was first recognized in southern Tibet within the contractional Himalayan orogen, having opposite sense of movement in contrast to the southward thrusting along the Main Central Thrust (MCT) (Burg et al., 1984; Burchfiel et al., 1992). Since then it has now been documented almost parallel to the Himalayan belt from Bhutan, Nepal and western Himalaya (Burchfiel and Royden, 1985; Herren, 1989; Burchfiel et al., 1992; Patel et al., 1993; Grujic et al., 1996; Hodges et al., 1996; Carosi et al., 1998; Dezes et al., 1999; Jain and Patel, 1999; Jain et al., 1999; Godin et al., 2006). Initially, it was interpreted as a thrust by the Chinese researchers (Academia Sinica, 1979).

The STDS corresponds to a series of north-dipping structures accommodating top-to-the-north

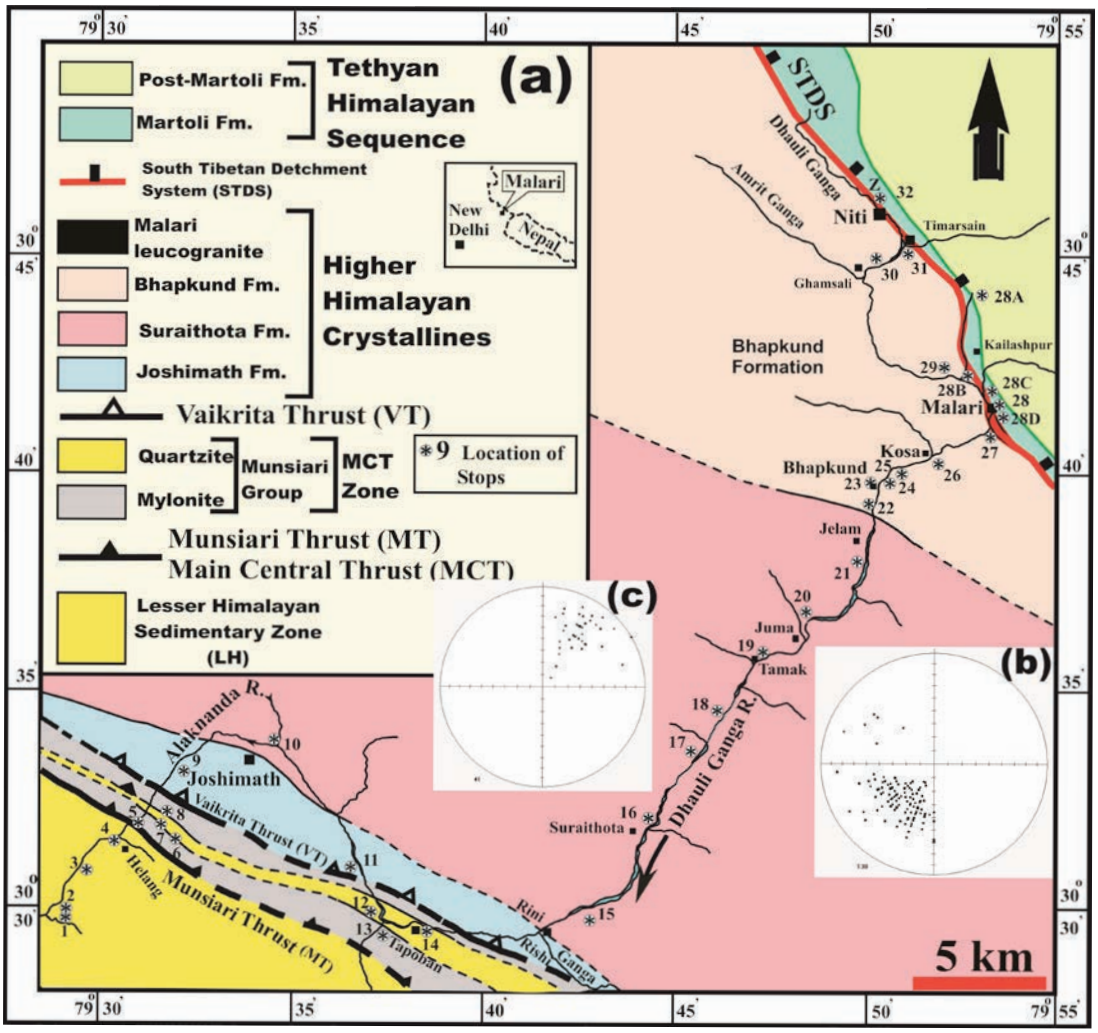

Figure 1
(A) Geological map of the Higher Himalayan Crystalline (HHC) Belt along the Alaknanda-Dhauli Ganga Valleys. Sources: Authors observations and other published literature. (B) Orientation data of 138 main foliation Sm plotted Equal Area Projection using GEOrient. (C) Orientation data of 41 lineations developed on main foliation Sm, plotted on Equal Area Projection using GEOrient. Location of stops shown as latitude and longitude, and original field locations in bracket.

normal motion of the Tethyan Himalayan Sequence (THS) in southern Tibet with respect to the underlying Higher Himalayan Crystalline (HHC) belt (Burchfiel et al., 1992; Burg, 1983; Burg et al., 1984). Normal motion has occurred on several ~ parallel low-dipping structures along the STDS that reveal from top to bottom (i) few brittle normal faults in the THS, (ii) a detachment at the contact between the unmetamorphosed to poorly metamorphosed THS and the underlying metamorphic rocks, and (iii) a ductile shear zone at the top of the HHC, the STDS shear zone, having highly deformed gneisses with NE-trending lineation and numerous shear structures indicating a normal motion (Leloup et al., 2010).

The main objectives of this work are to document some typical characters of the Cenozoic India-Asia convergence in the Uttarakhand Himalaya along a cross-section along the Alaknanda-Dhauli Ganga Valleys in a 6-day field excursion:

1. Characters, position and definition of the MCT vis-a-vis the Munsiari Thrust (the MCT–I), and the Vaikrita Thrust (the MCT–II),
2. Position and characters of the South Tibetan Detachment System (STDS),
3. Deformation of the HHC, and its detailed shear sense analysis,
4. Structural control on melt accumulation of the Himalayan migmatites,
5. Himalayan inverted metamorphism, and
6. Assessment of channel flow or other models that could try to explain the evolution of high grade metamorphic rocks and the processes involved in their exhumation.

GEOLOGICAL BACKGROUND

This section provides background on the major lithotectonic units and structures of the Garh-

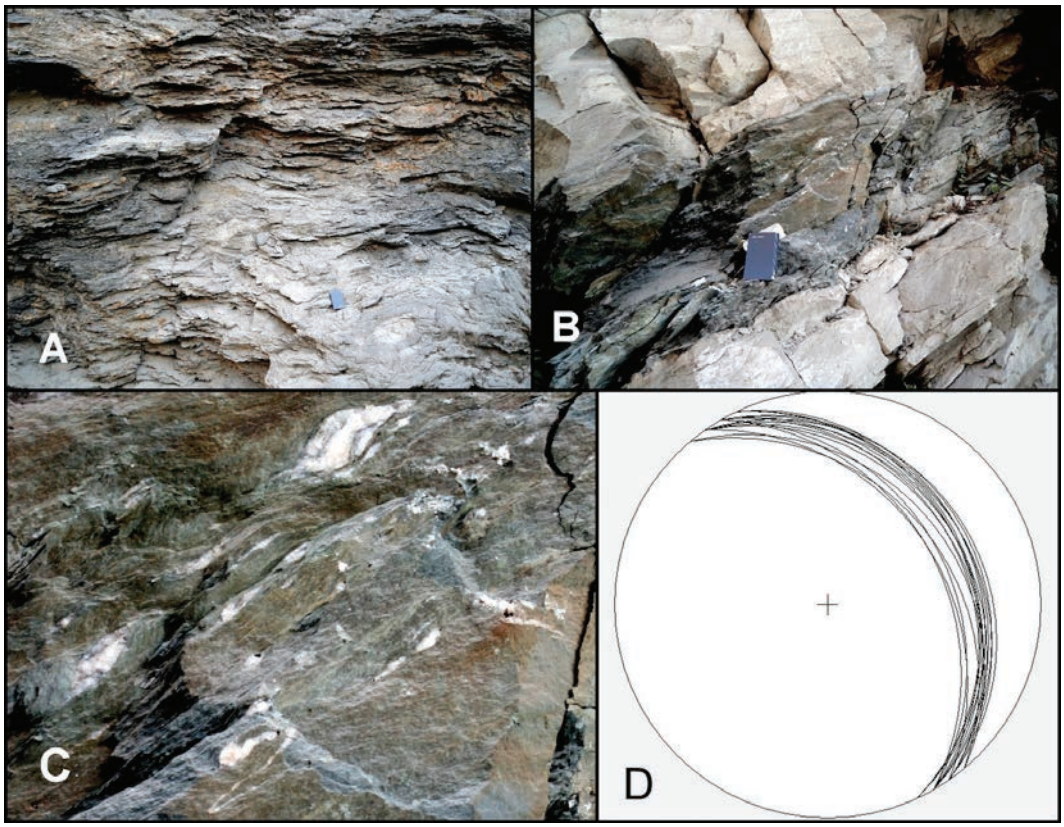

Figure 2
(A) Typical slate of the Lesser Himalayan Series sequence at Langsi. (B) Intercalated schist and quartzite. (C) Sigmoidal structure, S-C fabric and asymmetrical fold indicating shear sense, and (D) Stereo plot of main foliation Sm at the Stop – 1.

wal transect between Helang and Malari along the Alakhnanda-Dhauliganga valley in the Uttarakhand state of northwest India (Fig. 1). The transect begins with the low grade metamorphic rocks of Lesser Himalayan Sequence (LHS) near Helang, extends northward through the Main Central Thrust Zone rocks, high grade metamorphic rocks of the Higher Himalayan Crystallines and finally to the South Tibetan Detachment System and unmetamorphosed sedimentary rocks of the Martoli Formation near Malari. The Higher Himalayan Crystallines represent the highest grade, homoclinally north-east dipping metamorphic core of the Himalaya. This belt is bounded along its base by the Main Central Thrust (Heim and Gansser, 1939), now designated as the Munsiari Thrust in geological literature, and the South Tibetan Detachment System (STDS)/Trans-Himadri Fault (Valdiya, 1989, 2005; Valdiya and Pande, 2009) at the top. The mid crustal rocks of the HHC have been extruded out from beneath the Tibetan plateau and thrust southwards along the MCT (Beaumont et al., 2001, Jamieson et al., 2004) over the footwall of low grade metamorphosed and intensely foliated quartzite and phyllonite of the Lesser Himalayan Sequence near Helang. The STDS juxtaposes the unmetamorphosed sedimentary rocks of the Martoli Formation in the hanging wall with the sillimanite grade metamorphic rocks of the HHC near Malari. Based on the metamorphic grade and lithologies, the rocks of the HHC above Munsiari Thrust are divided into two groups: (1) the Munsiari Group in the lower parts and the (2) Vaikrita Group in the upper parts; separated by the Vaikrita Thrust (VT) (Gururajan and Chaudhuri, 1999).

The Main Central Thrust (MCT) was first recognized as the tectonic boundary between the monolithic northerly-dipping high grade High Himalayan Crystalline (HHC) Belt and the Proterozoic Lesser Himalayan (LH) sedimentary belt by Heim and Gansser (1939) and subsequently mapped by various workers along entire length of the Himalaya (Gansser, 1964; Hodges, 2000). Despite its occurrence across the Himalaya, precise identification and location of the MCT has been problematic in the field due to application of the following various criteria (see Searle et al., 2008 for review).

i. Presence of the ductile shear zones with different kinematics across the whole HHC and its emplacement over the LH along the MCT (Jain and Manickavasagam, 1993; Hubbard, 1996; Davidson, 1997).
ii. Identification of the MCT along a transition zone between the gneiss of the HHC and LH

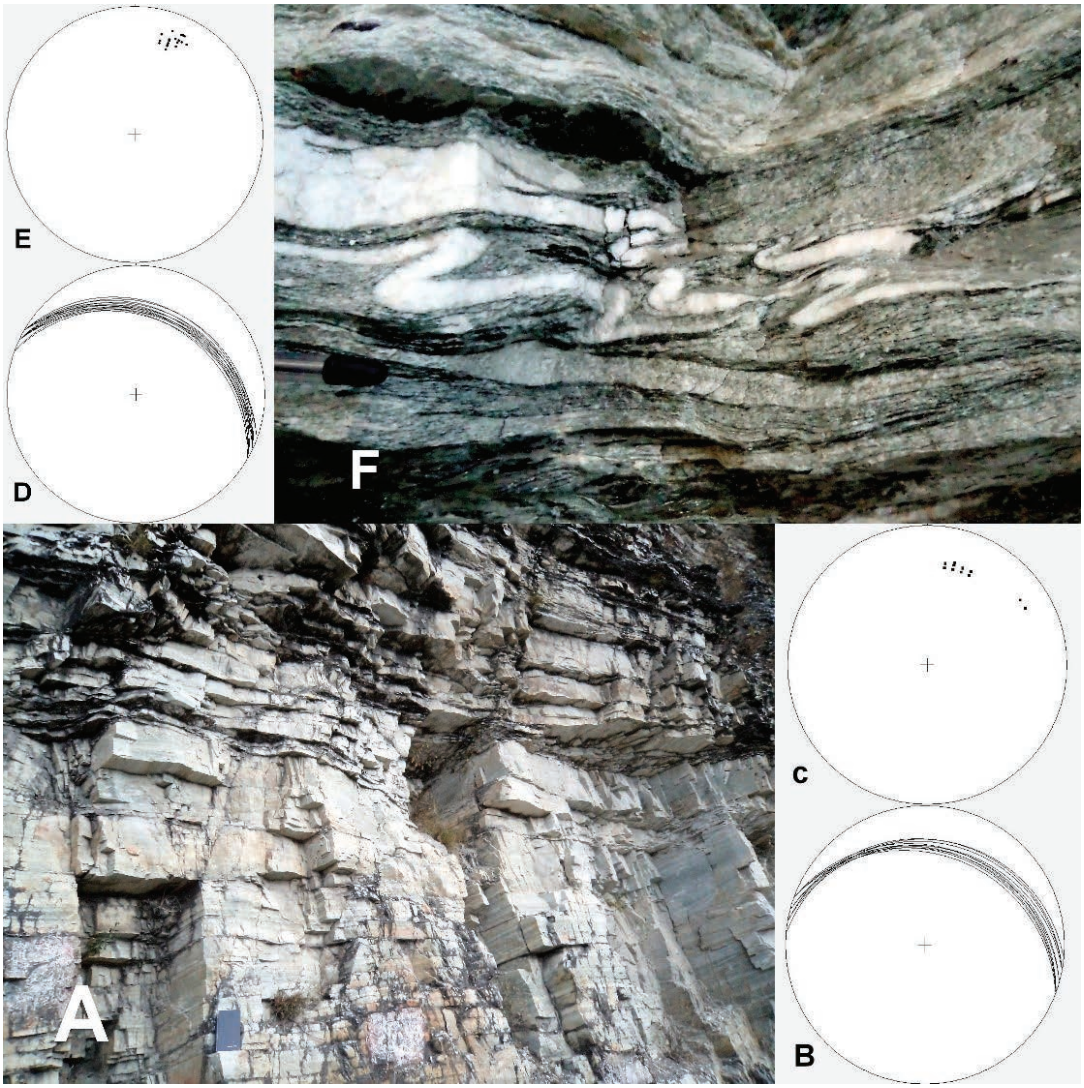

Figure 3
(A) Bedded and gently-dipping Lesser Himalayan quartzites. (B), (C), (D), (E) – Foliation and lineation data plotted on stereonet for Stops 2 and 3, respectively. (F) Asymmetrical folds in a narrow zone showing to top-to-the-SW sense shear.

sediments (Valdiya, 1980; Pecher, 1989).

iii. Distinct metamorphic break along the MCT (Vannay and Hodges, 1996; Valdiya, 1980).

iv. Distinct isotopic signatures within the HHC (Ahmad et al., 2000).

Valdiya et al. (1999 and references therein) identified an outermost crustal-scale mylonitized sheared package in the Uttarakhand Himalaya, bounded by the Munsiari Thrust (MT) along its base and the Vaikrita Thrust (VT) at its top. He separated the lower sequence of the Munsiari Formation from the Vaikrita Group by the latter thrust, and recognized the Vaikrita Thrust as the actual MCT (also Ahmad et al., 2000).

It is worthwhile to note that we use the term "formation" (a mainly stratigraphic term) for the deformed and metamorphosed rocks of the HHC with references to the large amount of existing consolidated bibliography even if the more correct term should be "unit" or "metamorphic complex".

Munsiari Group

Low- to medium- grade Munsiari Group is essentially made up of a highly imbricated and mylonitized Paleoproterozoic low to medium grade Munsiari Group rocks of dominant mylonitic augen gneiss [$^{207}Pb/^{206}Pb$ zircon age of 1848 ± 5 Ma from Jharkula – about 10 km west of Joshimath on main Rishikesh-Joshimath road and 1830 ± 6 Ma age from Tapovan (Wiedenbeck et al., 2014; Stop 8)] and fine grained biotite-rich gneiss, garnetiferous mica schist, phyllonite, sheared amphibolite, and a persistent imbricated horizon of sericite-bearing sheared and foliated quartzite; the latter bears a very strong lithological resemblance with the Lesser Himalayan Berinag Group

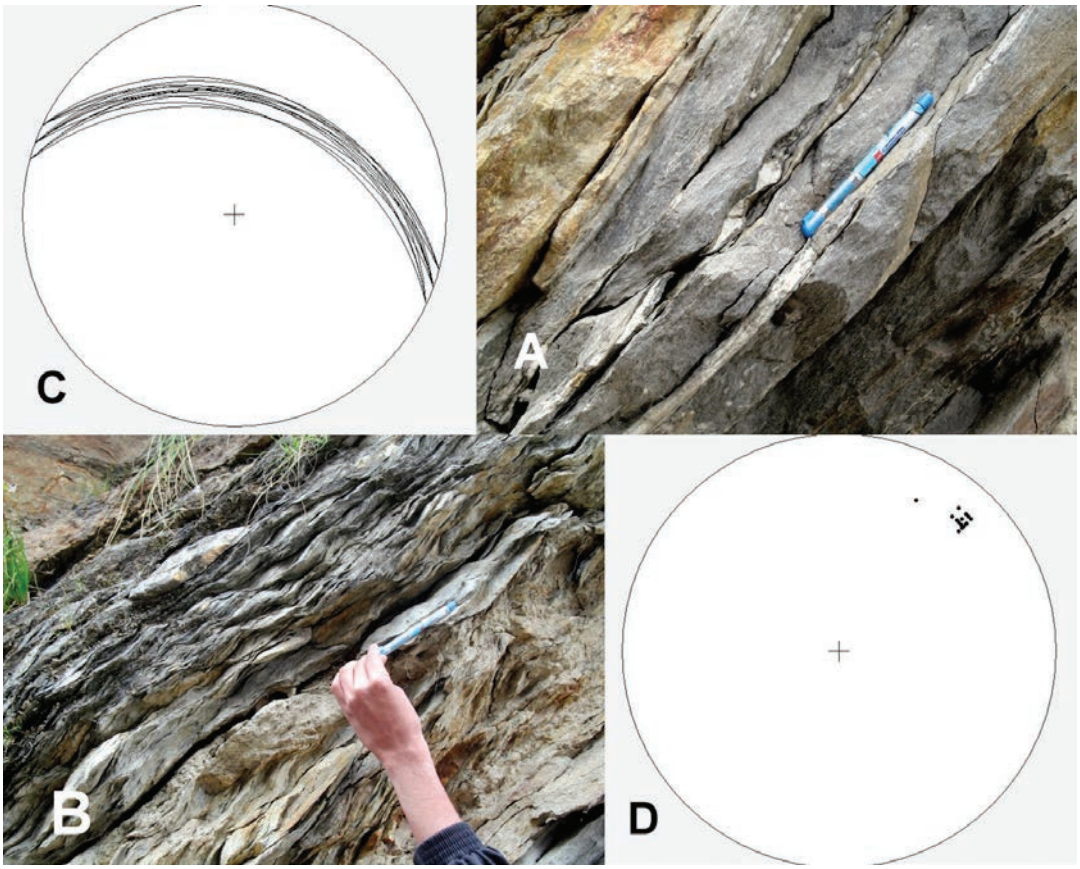

Figure 4
(A) Asymmetrically sheared boudin showing top-to-SW shear sense. (B) Iintercalated psammite/pelite schist with prominent S-C shear fabric. (C), (D) Foliation and lineation data of Location 4 plotted on stereonet, respectively.

quartzite. On the whole the rocks of this group display intense penetrative shearing. It is likely to have been incorporated within the basement Munsiari-type rocks due to imbricated Lesser Himalayan rocks. The pelitic samples within the Munsiari Group have mineral assemblage: quartz + biotite + plagioclase ± garnet ± staurolite + muscovite ± graphite ± andalusite (Spencer et al., 2012), while amphibolitic bodies have zoned calcic amphibole, plagioclase, quartz, biotite and minor epidote, opaque, chlorite and calcite. "Peak" pressure-temperature (P-T) conditions recorded by pelitic rocks increase structurally upward from 500 °C/0.5 GPa up to c. 580 °C/1.1 GPa (Spencer et al., 2012). According to Célérier et al. (2009) the Munsiari Group rocks have cooled to the white mica Ar-Ar closure temperature (350 ± 50 °C) at c. 9 Ma.

Vaikrita Group

The overlying Vaikrita Group sequence of the HHC within the lower and upper amphibolite facies is divided into three formations between the VT and the STDS: (1) the Joshimath Formation, (2) the Suraithota Formation, and (3) the Bhapkund Formation.

The Joshimath Formation comprises garnet-biotite-muscovite schist and psammitic/pelitic gneiss. Numerous quartz veins are seen within this unit, many of which have been isoclinaly folded. Geothermobarometric data by Spencer et al. (2012) indicated highest "Peak P-T conditions" conditions with respect to the previous formation with temperatures in spanning from c. 700 °C up to 830 °C and pressure of 1.0 to 1.4 GPa".

The Suraithota Formation comprises kyanite-garnet-biotite schist/psammitic gneiss and quartzites with thin amphibolite intercalations. Depositional features such as cross-beds are seen in less deformed rocks and indicate that many parts of this formation have been overturned. Pressure-Temperature values reported in the literature for this formation (referred by the previous authors as the Pandukeshwar formation) are in the range of c. 800-860 °C and c. 1.4 GP (Spencer et al., 2012).

The Bhapkund Formation comprises sillimanite (fibrolite)-garnet-biotite psammitic gneiss/schist, small tourmaline-rich leucogranite lenses/dykes and the Malari leucogranite body. Migma-

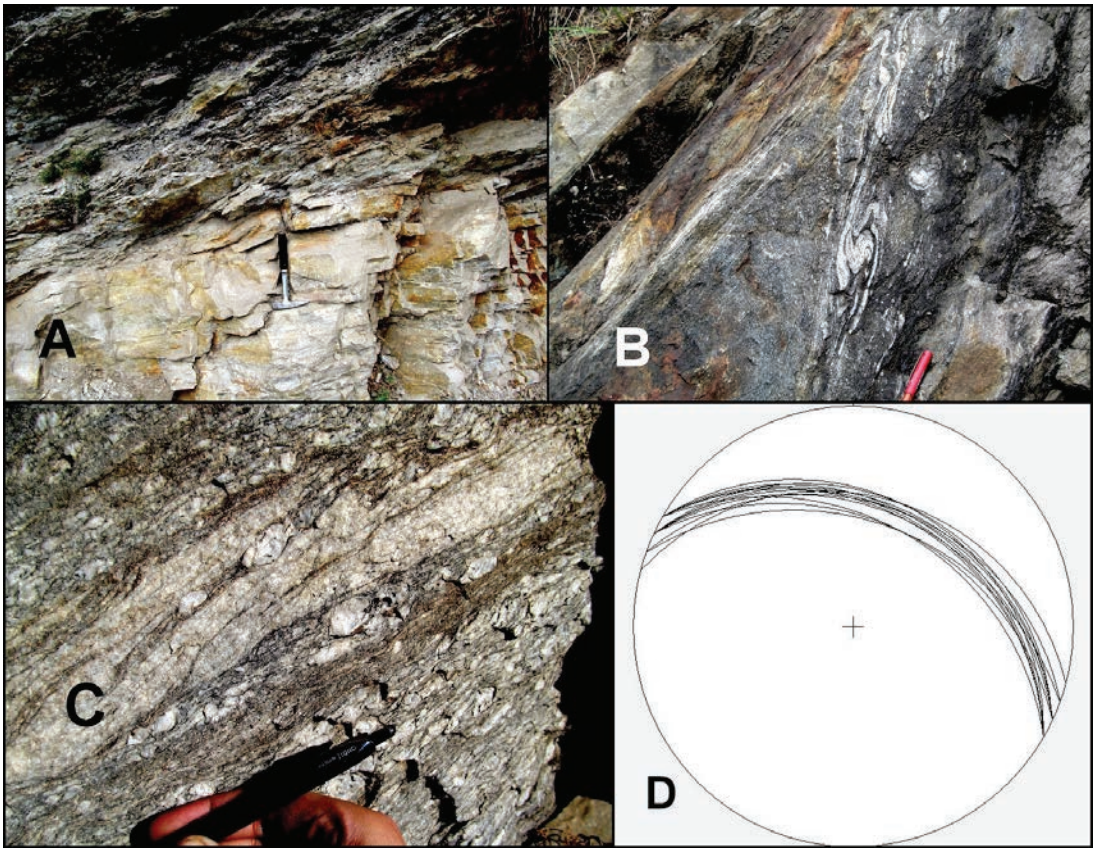

Figure 5
(A) Sharp contact between gneiss and quartzite at Stop 6. (B) Type-II superposed mushroom fold. (C) Megacrystic granite gneiss with grain size variation in the ductile shear zone. (D) Foliation data of garnetiferous mica schist of the Joshimath Formation at Stop 9, plotted on stereonet.

tization is pervasive within this formation. Phase equilibria constraints and geothermobarometry calculations by Spencer et al. (2012) reveal a pressure decreases from 1.05 GP to 0.85 GP towards the STDS in the the Bhapkund Formation (referred as the Badrinath formation), while the temperature is roughly constant (810-860 °C). A clear metamorphic break is present between the high-grade rocks of the Bhapkund Formation in the footwall of the STDS and the hanging wall low-grade to unmetamorphosed rocks of the Martoli Formation, where the maximum T of c. 450 °C has been qualitative estimated using phase equilibria arguments by Sachan et al. (2010).

Within the Vaikrita Group, metamorphic grade increases up the structural section (Jain et al., 2013), a phenomena called inverted metamorphism. This places the sillimanite–K-feldspar gneiss and migmatite of the Bhapkund Formation, which were metamorphosed under amphibolite facies at >650 °C, at the top (Sachan et al., 2010). Overall, the HHC trends NW-SE in this valley with dips of the main foliation Sm towards NE- to E. Various shear sense indicators proliferate between Helang and Malari. Asymmetric structures such as S-C and S-C' fabric, boudins, sigma structures, folds etc. provide valuable information regarding direction of tectonic transport. Top-to-south or southwest shear sense indicators are observed within the lower and middle parts of the HHC and top-to-north or northeast shear sense indicators are observed in the upper parts near the STDS.

Tethyan Himalayan Sequence

Martoli Formation

The basal Tethyan Himalayan Sequence (THS) is best exposed around the Malari village as the Martoli Formation, which dominantly contains greyish green slate and quartzite. Overall dip of the Martoli is towards N-to-NE. Other Paleo-Mesozoic formations of this sequence can be observed along the upper reaches of Dhauli Ganga and Birthi Rives.

FIELD EXCURSION

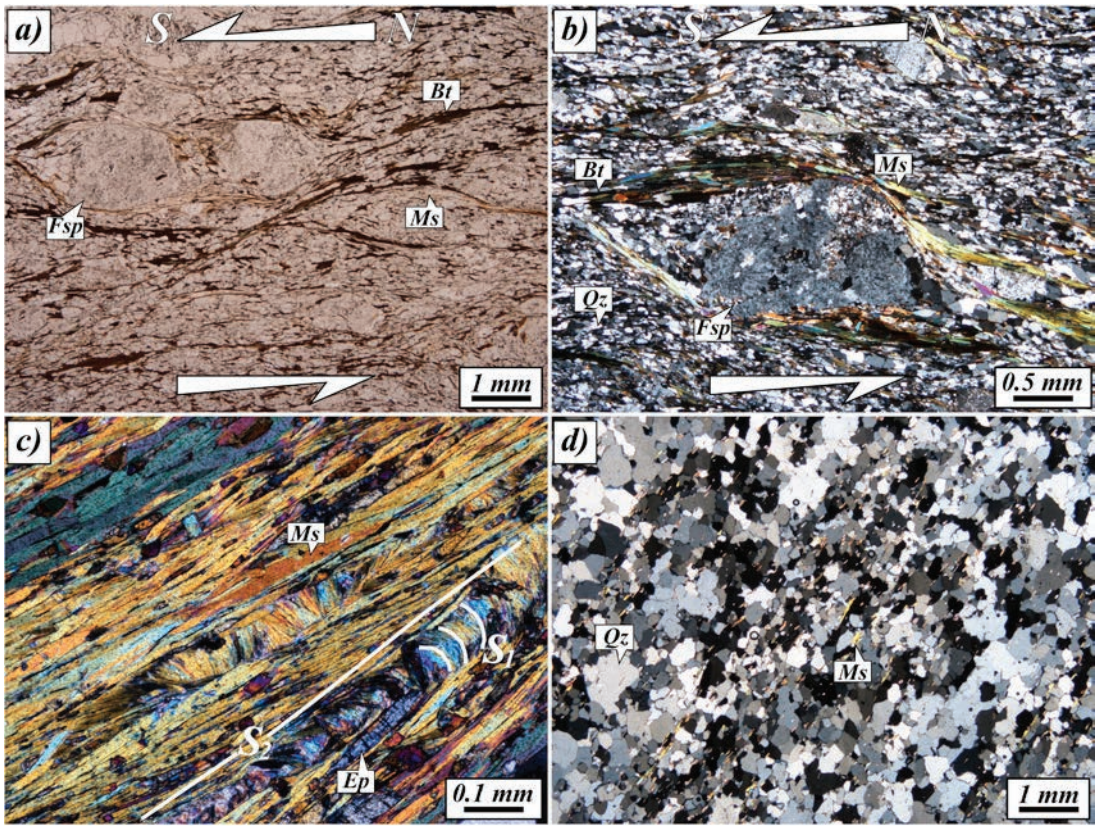

Figure 6
(A) S-C-C' fabric and feldspar prophyroclasts pointing a top-to-the-south sense of shear (mineral abreviations after Whitney and Evans, 2010). (B) Details of feldspar porphyroclast with asymmentric strain shadows in mylonite. (C) S1-S2 relationships within phyllite. (D) Continous foliation developed in quartzite.

Reaching Joshimath

All the foreign nationals may travel by air to Delhi/Dehra Dun and then to Haridwar either by train/road. This picturesque religious place, on the right bank of River Ganga, provides a glimpse of the Cenozoic foreland Middle Siwalik Group rocks. Next day involves a long road journey northeastwards for about 300 km upstream along the mighty Alaknanda River from Haridwar to Joshimath. Most of the journey is through the wide, meandering and picturesque Alaknanda River as one mostly travels through the Lesser Himalayan sedimentary sequence. Stay is at Joshimath, and since it is a long journey, it is suggested that the team takes rest on the first day when it reaches Joshimath and completes the formalties regarding permission etc. Since it is a restricted area near the border with Tibet, satellite phones and GPS are not permitted and under very strict servelliance by the Government of India for security reasons, hence you are advised not to use them at all and carry them beyond Joshimath. Field stops are numbered as Stops 1, 2 etc., while the original locations in our field research work are numbered as RM-, H- and T- series for co-ordination.

Starting the actual field excursion from the Joshimath camp, following are the day-wise detailed field visits and movement programme.

Day 1: Patalganga-Helang

The first day is devoted to critical observations along the Alaknanda River from the village Patalganga to Helang involving Proterozoic Lesser Himalayan Sequence (LH), its deformation and the MCT zone. One starts travelling across dominant lithology of the Lesser Himalayan quartzite belonging to the Garhwal Group/Berinag Group from the Patalganga village upstream along the Highway NH-58 northwards towards Helang through the villages of Langsi and Gulabkoti.

Stop 1

Locality: About 30 m south of Langsi. H-42 (N30°29'33":E79°29'1")
Theme: Lesser Himalayan Sequence (LH) and its deformation.

As one moves northwards from the Patalganga village towards Helang, typical slate of the Lesser Himalayan Sequence can be observed (Fig. 2A), which are intercalated with light-colored foliat-

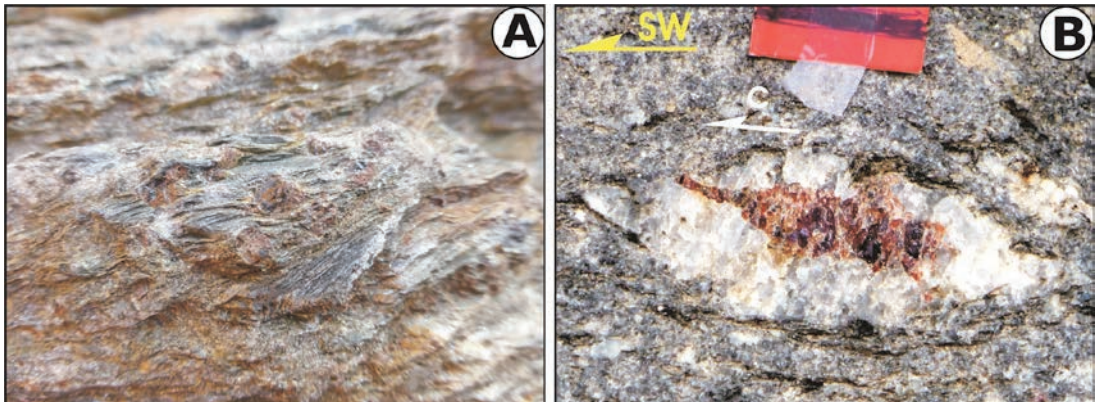

Figure 7
(A) Gently-dipping garnet-biotite schist at Stop 9 of the Joshimath Formation. Note asymmetrical garnet augen with tails of the foliated rock, indicating top-to-the-SW shear sense. (B) Tailed garnet asymmetrical porphyroblast in kyanite-garnet gneiss within the Suraithota Formation at Vishnuprayag showing top-to-the SW shear sense. Scale: 2 cm.

ed as well as massive quartzite throughout from Langsi to Helang (Fig. 2B). The LH sequence strikes almost NW-SE and dip about 33° NE (Fig. 2D). Sigmoidal σ-shaped veins, S-C shear fabric and rootless folds reveal a consistent top-to-the-SW upwards shear sense in the Lesser Himalayan Sequene much farther south from the MCT (Fig. 2.1C).

Stop 2

Locality: About 500 m north of Langsi. H-40 (N30°29'51":E79°29'5")
Theme: Lithology of the Lesser Himalayan quartzite.

A huge exposure of typical cliff-forming light-colored Lesser Himalayan Garhwal Group quartzite can be observed at this stop (Fig. 3A). The rocks show a shear sense of top-to-the SW and are highly foliated. The quartzites strike about NW-SE and dip 30° due N to NE (Fig. 3B). The strong sericite and quartz mineral lineation in the quartzite plunges N15° at about 25° (Fig. 3C).

It is worthwhile mentioning that dominant lithology in this part of the Lesser Himalayan Sequence is still quartzite, though there are intercalations of highly deformed and foliated schist within the quartzite.

Stop 3

Locality: About 350 m north of Gulabkoti. H-32 (N30°30'48":E79°29'33")
Theme: Rootless folds in the Lesser Himalayan quartzite.

Another excellent exposure of the Lesser Himalayan quartzites is observed at this stop. The quartzite strikes nearly WNW-ESE and dips 35° NE (Fig. 3D), while the lineation is oriented N20°/30° (Fig. 3E). Asymmetrical folds having sheared and appressed limbs with a top-to-the-SW shear sense are also observed in the highly deformed schist (Fig. 3F).

Helang-Joshimath

In the afternoon of Day 1 field work is focused on the Munsiari Group rocks of the MCT zone. This is critical for understanding the relationship between Munsiari and Vaikrita Thrusts in this region. For this purpose, detailed observations are made along the main Highway NH-58 between Helang and Joshimath and along a side road that bifurcates to Shelang village.

Stop 4

Locality: About 250 m south of Helang Bridge. RM-35/H-26 (N30°31'32":E79°30'30")
Theme: Deformation within the MCT zone.

After observing the Lesser Himalayan quartzites south of the village Helang, one moves further northwards, where psammite is interbanded with schist; both are more strained. Magnificent S-C-C' fabric in the form of asymmetrically sheared boudin (Fig. 4A) is observed at this exposure indicating a top-to-the-SW shear sense. Near this stop, one can observe typical S-C shear fabric affecting the intercalated psammite/qtz-bio schist (Fig. 4B). The schist, in general, strikes about W-E to NW-SE and dips 43° N to NE, and a strong mineral lineation plunging down-the-dip. The grade of metamorphism in this region is distinctly higher as compared to the southern parts of the Alaknanda Valley.

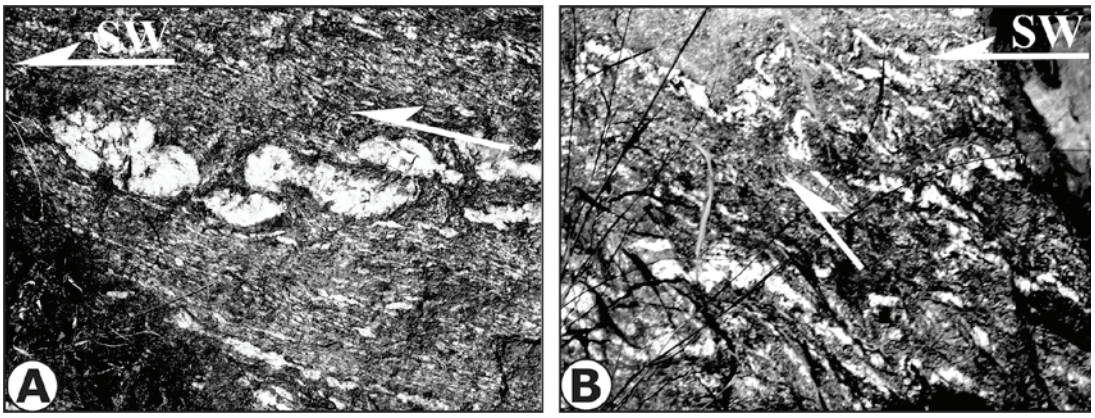

Figure 8
(A) Folded and boudinaged quartz vein in psammatic gneisses of the Joshimath Formation at Stop 11. Shear zone moves part of vein SW. (B) Close asymmetrical folds indicating top-to-the-SW asymmetry. Loc. Stop 11.

Stop 5

Locality: About 2 km NE from Helang village. RM 37/H-22 (N30°31'50":E79°30'53")
Theme: Mylonite of the Munsiari Group.

The first exposure of mylonitized gneiss along the Munsiari Thrust, and hence the beginning of the Munsiari Group is observed at this stop. The mylonite is coarse-grained megacrystic gneiss. High strain deformation, as typical of a mylonite, is observed and S-C fabric is well-developed indicating a top-to-SW shear sense. The intensely sheared mylonite strikes nearly W-E to NW-SE and dips 45° N to NE (Fig. 4C). A prominent stretching lineation is observed with a plunge of N20°/45° (Fig. 4D). This sudden increase in deformation in the rocks and presence of a granite mylonite suggests a major break in the litho-sequence indicating a major thrust – the Munsiari Thrust.
It is important to point out that, as we move north for about 2 km, a thick quartzite band is observed which has a strike continuity up to Tapovan.

Stop 6

Locality: About 3 km ESE on the side road. RM-45/RM-119 (N30°31'42":E79°32'18")
Theme: Quartzite of the Lesser Himalayan within an imbricate zone.

A sharp contact with the dark augen mylonite gneiss overriding the LH quartzite (Fig. 5A) is observed at this stop. This contact is possibly an out-of-sequence thrust which has caused a repetition in the quartzite-mylonite sequence. The gneiss above the contact strikes almost E-W and dips 30° to the N, whereas the quartzite below the sharp contact strikes WNW-ESE to NW-SE and dips 20° N to NE. An angular discordance is distinct between the two sequences.

A variety of magnificent structural features like Type-II superposed mushroom folds (Fig. 5B) and S-C-C' fabric are observed at this outcrop. The shear sense, as indicated by the S-C fabric and the folds, is top-to-SW. There is intense localization of deformation and shearing at the rocks contact.

At the microscale, the foliation in the gneiss is associated with the dynamic recrystallization of muscovite, biotite and quartz and it is a spaced anastomosing foliation (Passchier and Trouw, 2005). Kinematic indicators are represented by S-C-C' fabric (Fig. 6A), mica and biotite fishes referable to type 1 and 3 of Passchier and Trouw (2005) and asymmetric pressure shadows around porphyroclasts (Figs. 6A, B). Within the phyllitic layers an older foliation is still recognizable (Fig 6C). In the quarzites layers a continous foliation is defined by the preferred orientation of platy minerals such as chlorite and white mica. The granoblastic quartz matrix, shows evidence of dynamic recrystallization (GBM I of Stipp et al., 2002a, b). Gypsum plate observations also suggest a strong LPO (lattice preferred orientation) in such quartzite.

Stop 7

Locality: On the side upper road from Jharkhola towards SE. RM–39/H–11 (N30°31'52":E79°31'47")
Theme: Mapping of the Lesser Himalayan quartzite band.

After the observation of the sharp contact between the light-colored quartzite and the dark-colored gneiss, one may move further north along the road, where a repetition of the light-colored quartzite similar to the Lesser Himalayan quartzite is observed. These quartzites are highly foliated and continue along the strike up to Tapovan vil-

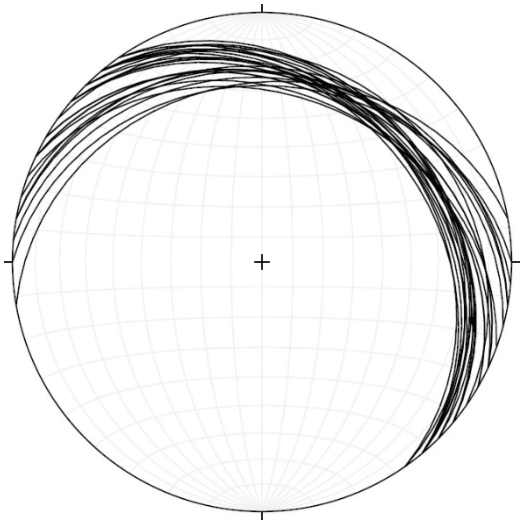

Figure 9
Main foliation within the Joshimath Formation at Stop 11 and nearby areas.

lage. The quartzites strike E-W to NW-SE and dip about 35-40° N to NE. Rootless folds indicating a top-to-SW shear sense and transposed foliation can also be observed at this outcrop. The lineation plunges around N25°/30°.

Stop 8

Locality: Near Jharkhola. RM–120 (N30°32'3":E79°32')
Theme: Mylonite of the Munsiari Group rocks.

After moving further north of the quartzite band, fine-grained as well as coarse-grained megacrystic mylonite is observed at this stop. The mylonitized rocks strike about E-W and dip 30-35° to the N, and a strong lineation develops plunging N15°/40°.

At this stop one can clearly observe a ductile shear zone, evidenced by grain-size variation due to development of alternating ultramylonite bands (Fig. 5C). The mylonitic rocks observed at this stop have the typical lithology of the Munsiari Formation. Wiedenbeck et al. (2014) performed a Cameca ims 4f ion probe $^{207}Pb/^{206}Pb$ analysis on extracted zircon crystals from this mylonite and obtained a weighted mean age of 1848 ± 5 Ma indicating the age of crystallization of this granitoid protolith, though the age of mylonitization/thrusting along the MCT/Munsiari Thrust remained unconstrained.

Stop 9

Locality: About 10 km north of Helang. RM–46/ RM–124 (N30°33'14":E79°32'25")
Theme: Into the Vaikrita Group

As one moves along the main road further north from Stop 8, a drastic change in lithology is observed from intensely sheared mylonite gneiss to garnetiferous mica schist, suggesting that one has entered into the Joshimath Formation of the Vaikrita Group. The first good exposure of garnet-biotite schist/gneiss, typical of the Joshimath Formation, is observed at this stop (Fig. 7A). The garnetiferous mica schist and garnet-biotite gneiss strikes WNW-ESE to NW-SE and dips 35-40° N to NE (Fig. 5D) and the sense of shear in these rocks is top-to-the-SW.

Day 2: Joshimath-Suraithota

Day 2 involves journey from Joshimath to Suraithota along the Dhauli Ganga River (Fig. 1). Before proceeding to Suraithota, it is better to observe typical Suraithota Formation at Vishnuprayag first by descending to the confluence of the Akalnanda and Dhauli Ganga Rivers. The section first cuts back into the Munsiari Group rocks through the Joshimath Formation rocks, and then back again to the Joshimath Formation. Thus, the Vaikrita Thrust is observed twice along the same road section. The Joshimath Formation finally grades into the psammatic gneiss of the Suraithota Formation. The objective is to (i) locate the Vaikrita Thrust, (ii) carry out detailed analysis of the shear sense indicators, (iii) locate the contact between Joshimath and Suraithota Formations, and (iv) observe the lithology characterizing each formation. The traverse is about 40 km.

Stop 10

Locality: Vishnuprayag bridge. RM 48 (N30°33'54":E79°34'36")
Theme: Garnet porphyroblast in the kyanire-bearing Suraithota Formation

This stop is located on the Joshimath-Badrinath sector of the highway at Vishnuprayag – the confluence of the Alaknanda and Dhauli Ganga Rivers, and the place where the former cuts a deep gorge through the Suraithota Formations and becomes almost invisible. As Joshimath and its surroundings habitat are located on a huge paleolandslide zone, exposures are extremely poor till one completes all the loops and approaches

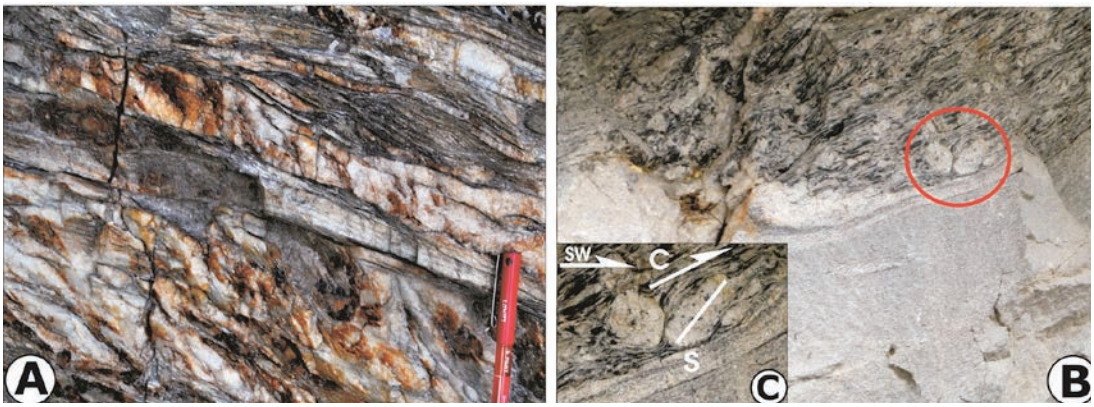

Figure 10
(A) Imbricated Lesser Himalayan quartzite within the MCT zone showing highly sheared quartzite with sub-horizontal ductile shear zones. Stop 12, west of Tapovan. (B) Very coarse megacrystic asymmetrical feldspar embedded in sheared biotite-rich foliated matrix of the Munsiari-type augen granite mylonite in the MCT shear zone. Mylonite is traversed obliquely by foliated and younger aplitic gneiss. (C) Insert shows distinct S-C shear fabric and asymmetric σ-type augen, having top-to-the-SW shearing. Stop 13 along Dhak Nala. See text for isotopic data.

the banks of the Alaknanda River. On either side one encounters flaggy psammitic gneiss of the Suraithota Formation, which is best exposed on the right bank of the river. As one approaches the bridge on the Alaknanda River, kyanite-bearing garnetiferous mica schist and gneiss dip into the hill and run almost parallel to the river course. Syntectonically-grown asymmetrical garnet porphyroblast in the porphyroblastic kyanite-bearing garnetiferous mica gneiss/schist of the Suraithota Formation is embedded within quartz (Fig. 7B).

Stop 11

Location: Barhgaon on the NH 58. RM–129 (N30°31'27":E79°36'00")
Theme: Folds in Joshimath Formation.

Typical gneisses of the Joshimath Formation are best exposed along the NH58 road section few kilometres southeast of the Joshimath town after crossing the scree and bad road patch. Quartz veins acquire augen shapes within these gneisses and are discretely sheared (Fig. 8A). Asymmetrical close folds possess steeply-dipping axial surfaces where small amount of movement is recorded indicating top-to-the-SW vergence (Fig. 8B). The rocks of this sequence strike E-W to N325° and dip about 25°-32° towards N (Fig. 9). Lineation trends N50°-65° and plunges down the dip 20°-30°.

Stop 12

Locality: About 2.50 Km WNW of Tapovan on the NH 58. RM–71 (N30°30'10": E79°36'52".
Theme: Imbricated Lesser Himalayan quartzite

Before encountering the Lesser Himalayan quartzite at Tapovan, one traverses through the mylonite, pelite/psammite and garnetiferous schist of the upper Munsiari Formation. Thus, the Vaikrita Thrust is located in this region, and has caused intense ductile shearing of the rocks with the development of S-C fabric showing top-to-the southwest movements and shear-bound intrafolial folds.

The imbricated Lesser Himalayan quartzite is again exposed along the strike on the road where it descends to the picturesque bower-shaped valley of Tapovan. Intense ductile shearing characterizes the exposure of strongly foliated quartzite, possibly due to the presence of the Vaikrita Thrust (Fig. 10 A).

Stop 13

Locality: About 0.75 Km W of Tapovan on the NH 58. RM-68 (N 30°29'28":E79°37'28")
Theme: Megacrystic Munsiari-type mylonite.

After crossing the Dhak Nala before approaching Tapovan, an interesting sequence of highly sheared megacrystic mylonite, deformed foliated aplite, amphibolite and schist is exposed, belong-

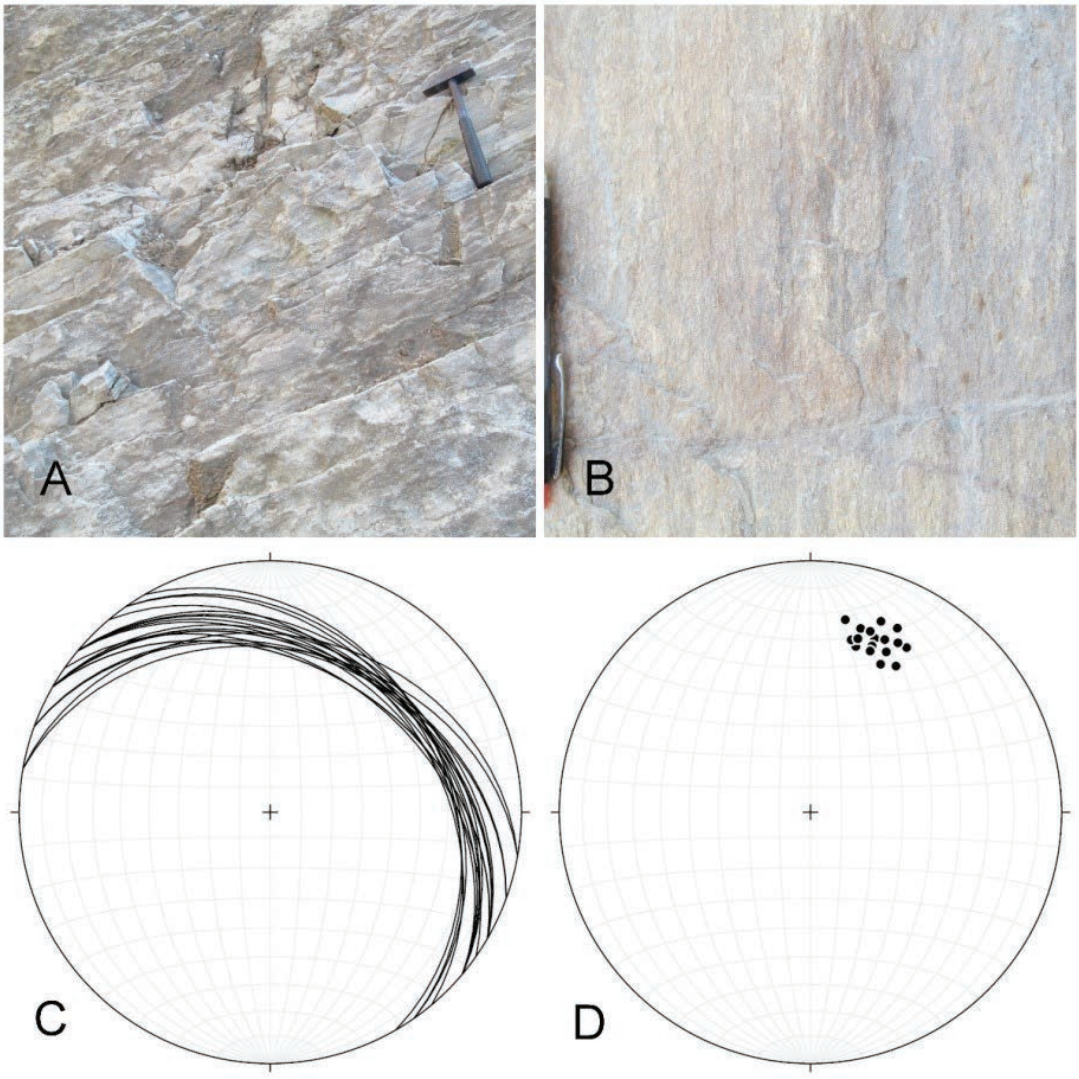

Figure 11
(A) Typical foliated quartzites seen near Tapovan at Stop 14. (B) prominent N-NE trending lineation in quartzites. (C), (D) Stereonet plots of the foliation and lineation, respectively.

ing to the typical Munsiari-type mylonites. More rigid porphyroclast within the mylonite consists of central sigmoidal-shaped single crystal within highly sheared fine-grained foliated matrix (Figs 10B, C). They typically develop from more resistant feldspars in a strongly foliated quartz, feldspar and mica matrix in sheared granite mylonite. In course of deformation the porphyroclasts develop asymmetric recrystallized tails showing stair stepping geometry (Fig. 10C). Most common porphyroclast is σ-type whose asymmetry and stair stepping define the shear sense towards top-to-the-SW (Figures 10 B). Rarely δ – type tails are also seen; both of them are useful in shear sense determination. Overall the mylonites strike N280° and dip 30° towards N.

$^{207}Pb/^{206}Pb$ analysis on extracted zircon crystals from an augen gneiss, possibly this megacrystic mylonite (Wiedenbeck et al., 2014), cross-cutting the biotite gneiss yielded a weighted mean age of 1830 ± 6 Ma indicating the younger limit for crystallization of this porphyritic dyke, though the age of mylonitization/thrusting along the MCT/Munsiari Thrust remained unconstrained. Field relations at this particular locality clearly points out still younger granite phases within the Munsiari Group rocks.

Stop 14

Locality: Tapovan Hot Spring. RM–66 (N 30°29'12", E79°39'12").
Theme: Imbricated Lesser Himalayan quartzite

This stop at the Tapovan Hot Spring exposes the intensly sheared and imbricated flaggy quartzite

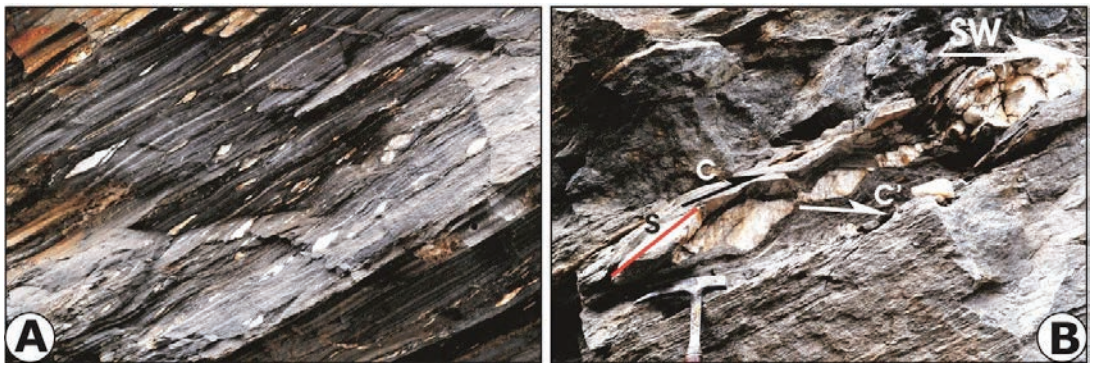

Figure 12
(A) Strings of sheared quartz veins transposed along NE-dipping shear zones in dark psammitic schist of the Suraithota Formation along the main foliation Sm. Stop 15. (B) Asymmetrical shear boudins from the Suraithota Formation, bounded by C and C' planes, indicating top – to – SW thrust-type shear shear sense.

within the MCT zone (Fig. 11A) along the strike where it is very strongly foliated and lineated (Fig. 11B). The quartzite strikes N280°-N320° and dips at about 35° towards NE (Fig. 11C). Lineation in quartzite is highly conspicuous and has N30°/30° orientation (Fig. 11D).

Stop 15

Locality: About 5 km SW of Suraithota on NH 58. Loc. RM 58 (N30°29'45":E79°43'00")
Theme: Lithology of the Suraithota Formation

As one traverses further upstream along the Dhauli Ganga Valley from Tapovan one crosses the Munsiari-type mylonite, the Vaikrita Thrust and Joshimath Formation again due to their strike continuity. The Vaikrita Thrust appears to be located within scree, till and fault gauge which preclude any direct observation of this boundary. Mylonitzation is pervasive below the Vaikrita Thrust. It is only after crossing the Rishi Ganga at Rini a distinct gradual change in lithology is noticed where dark coloured flaggy psammitic gneisses are intercalated with schist (Fig. 12A). In the lower parts typical Suraithota rocks are kyanite-garnet-biotite gneiss/schist, psammitic gneiss and thin calc-silicate layers with amphibolite. Rectangular or lozenge-shaped asymmetric boudins, displaced by interboudin surfaces at regular intervals, characterize these rocks and reveal top-to-the-SW (thrust) shear sense at this locality (Fig. 12B).

Lithology at this stop is characterized by garnet-biotite-muscovite (± staurolite) schist, psammitic/pelitic gneiss and granitic gneiss. The gneisses are typical of the Joshimath Formation with thin psammite bands similar to those of the Suraithota formation. Thus, the contact between the Joshimath and Suraithota formations is gradational, and makes it difficult to map very precisely in the field. Psammitic component increases northeastwards. The strike of the main foliation is N300°-N330° with a dip of 30°-40°. Lineation trends about N40° and plunges 30°. Shear sense indicators consistently show a top-to-the southwest movement.

At the microscale, mylonitic gneiss of the Vaikrita Thrust show an anastomosing disjunctive cleavage, with sporadic preservation of an older foliation, now transposed. Within the Joshimath Formation, mineral assemblage is made by garnet, white mica, biotite, quartz, plagioclase, staurolite, and minor opaque, tourmaline, zircon and monazite. Staurolite porphyroblasts are aligned on the main foliation, and when an internal foliation (Si, made by quartz, opaques and micas) is present, it is continuous with the external one. This observations led to the interpretation of staurolite as a synkinematic porphyroblast (Fig. 13B). Garnets have also an internal helicitic foliation (Si) that changes from discontinous to continous respect to the external one. In the latter case, the rotation of Si, suggests a sense of shear compatible with other independent kinematic indicators (see below). In this framework garnet could be interpretated as early to synkinematic mineral. Minor retrogression of garnet in aggregate of white mica, biotite and plagioclase is present (Fig. 13C), while white mica and minor chlorite partially pseudomorphosed on staurolite are widely observed. Well-developed kinematic indicators are present, such as S-C-C' fabric (Fig. 13A), mica fishes, drag folds and asymmetric mantled porphyroclast and asymmetric strain shadows around porphyroblast (Fig. 13C), pointing a top-to-the-south sense of shear. Quartz has undulose extinction and irregular grain boundaries. By the way stain free grains and straight grain boudaries are also common suggesting that a process of annealing (GBAR) should also be present, after the dynamic recrystallization (Fig. 13A). At times, relict S1 foliation is preserved between mica-rich second foliation S2 indicating that transposion of an earlier folia-

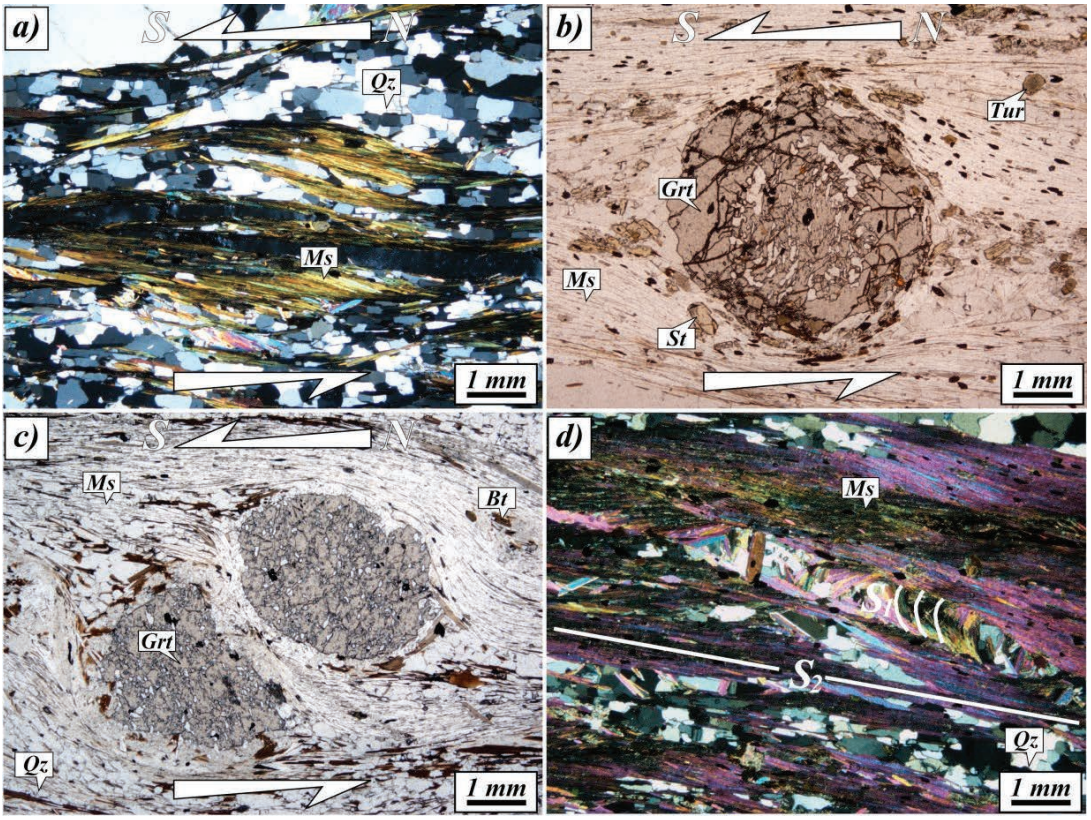

Figure 13
(A) S-C shear fabric, defined by muscovite and quartz in mica schist of the Joshimath Formation (JF). (B) (Early?) syn-tectonic garnet porphyroblast with staurolite and minor tourmaline in sheared mica schists of the JF (C) Asymmetric strain shadows around garnet. (D) Main (S2) foliation overprinting the older (S1) foliation.

tion is almost complete (Fig. 13D).

Day 3: Suraithota to Juma

Day 3 involves covering the central parts of the Higher Himalayan Crystallines (HHC) between Suraithota and further northeast. As proper camping facilities are not available in this part of the section for a larger group of investigators and distance from Joshimath increases, it would be advisable to change camp and establish it in the vicinity of Malari, either at the PWD Guest House or some suitable locality further north. The main section in this traverse covers (i) typical lithologies of the Suraithota Formation, (ii) mapping and deleating parts of the section revealing top-to-the SW shear sense, and (iii) its changeover to the top-to-the NE shear sense, (iv) the zone of transition of the changeover, and finally (v) the appearance of migmatite.

Stop 16

Locality: About 1 km NE of Suraithota after crossing the bridge. RM–81 (N30°32'31": E79°44'26")
Theme: Calc-silicate bands

Psammitic gneiss and thin garnet-muscovite-biotite schist intercalations dominate the Suraithota Formation in the lower middle parts, having thin isolated calc-silicate bands containing garnet, pyroxene and amphiboles (Fig. 14A). Fine-grained gneiss contains asymmetrical quartz and foliation boudins (Fig. 14B); both exhibiting top-to-the SW ductile shear sense parallel to the main foliation, which strikes N290° and dips 300°NE with a strong down-the-dip plunging mineral lineation.

Stop 17

Locality: About 3.5 km NE of Suraithota. RM–84 (N 30°33'34":E 79°45'43")
Theme: Identification of shear indicators and appearance of Top-to-NE shear sense

The first evidences of the top-to-the-NE shear sense within the HHC are encountered much to the southwest of the STDS as shear bands where foliated psammitc gneiss of the Suraithota is sigmoidally bent along the shear zones (Fig. 15A). These bands mostly strike N320° and dip mostly between 35 and 60° NE.

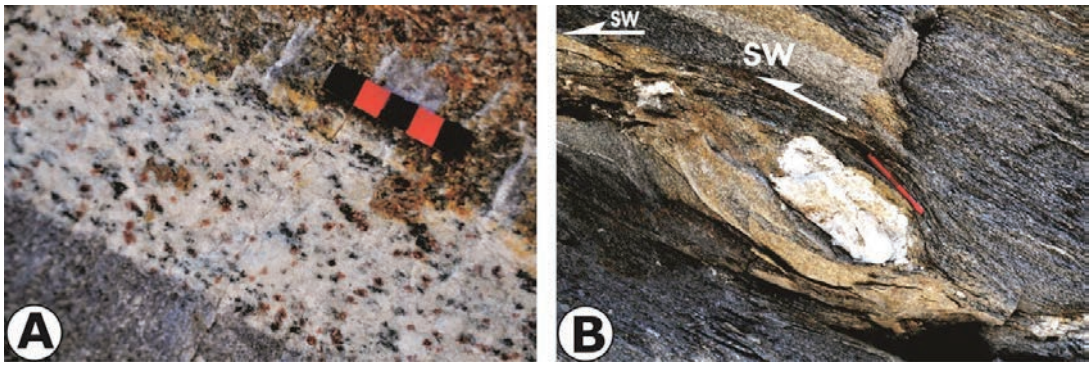

Figure 14
(A) An isolated calc-silicate layer within psammitic gneiss containing garnet, pyroxene and amphibole porphyroblasts within calcite-rich and poorly-foliated groundmass. (B) Asymmetrical quartz boudin within large-sized foliation boudin in fine grained gneiss; both exhibiting top-to-the-SW shear sense.

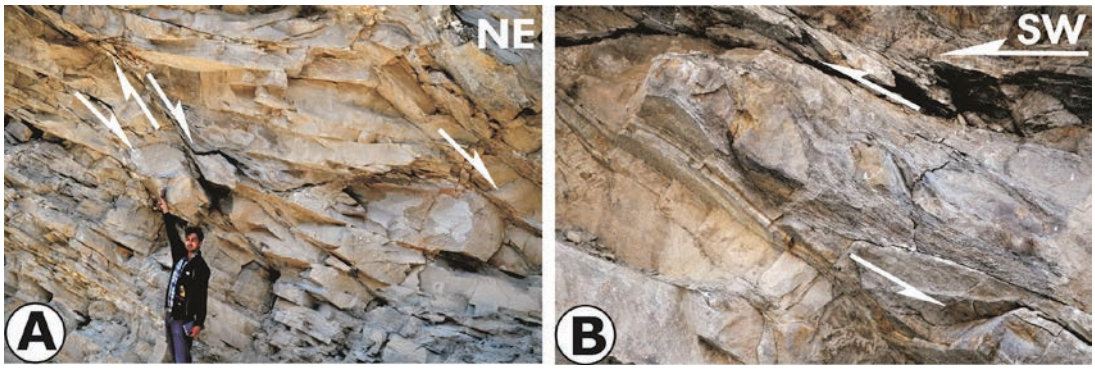

Figure 15
(A) Top-to-the-NE shear sense indicators as shear bands at Loc. RM–84. (B) Rootless isoclinal folds within a shear zone showing top-to-the SW shear sense at Loc. RM–86. Scale: Photo length about 2 m.

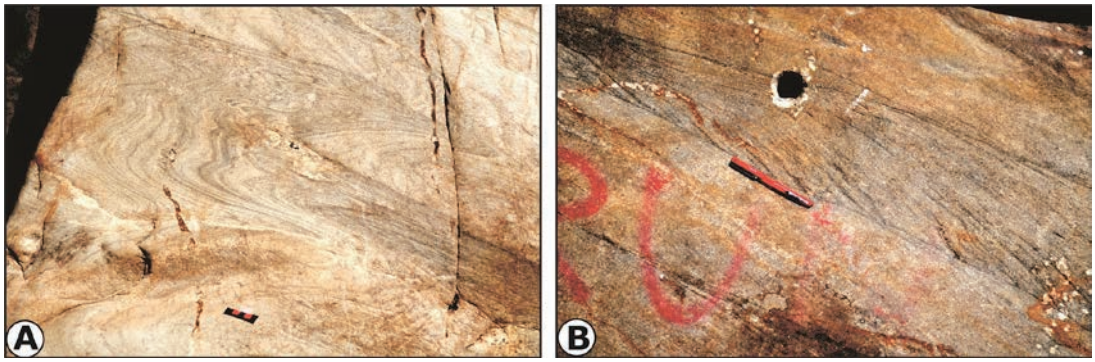

Figure 16
(A) Large-scale flowage of quartzo-feldspathic gneiss at Stop 19 near Tamak. (B) Inverted trough cross-beds.

Stop 18

Locality: About 5 km NE of Suraithota. RM–86 (N30°34'12":E79°46'22")
Theme: Ductile shear zones within the HHC

Near the upper parts of the Suraithota Formation, psammitic gneiss, quartzite and schist predominate with intercalated quartzite bands isoclinally folded and exhibiting considerable flowage from their limbs (Fig. 15B). Obliquely trending axial surfaces are sigmoidally bent due to top-to-the-SW ductile shearing, thereby indicating the presence of both the shear sense within the HHC. Main foliation withing the sequence strikes N290° and dips 250°N.

Stop 19

Locality: Tamak village. RM–88 (N 30°35'48":E 79°47'26")
Theme: Flow structures within quartzo-feldspathic gneiss of the HHC

After crossing Tamak and its tributary a zone of about 1.5 km is exposed which lacks any shear sense indicators. Instead, it exhibits extensive isoclinal to tight well-developed folds in quartzo-feldspathic gneiss (Fig. 16A). River scouring and erosion has smoothen the rock surfaces so much that it is difficult to know their orientations. Beautiful inverted trough cross-beds represent that parts of the HHC sequence are at least lo-

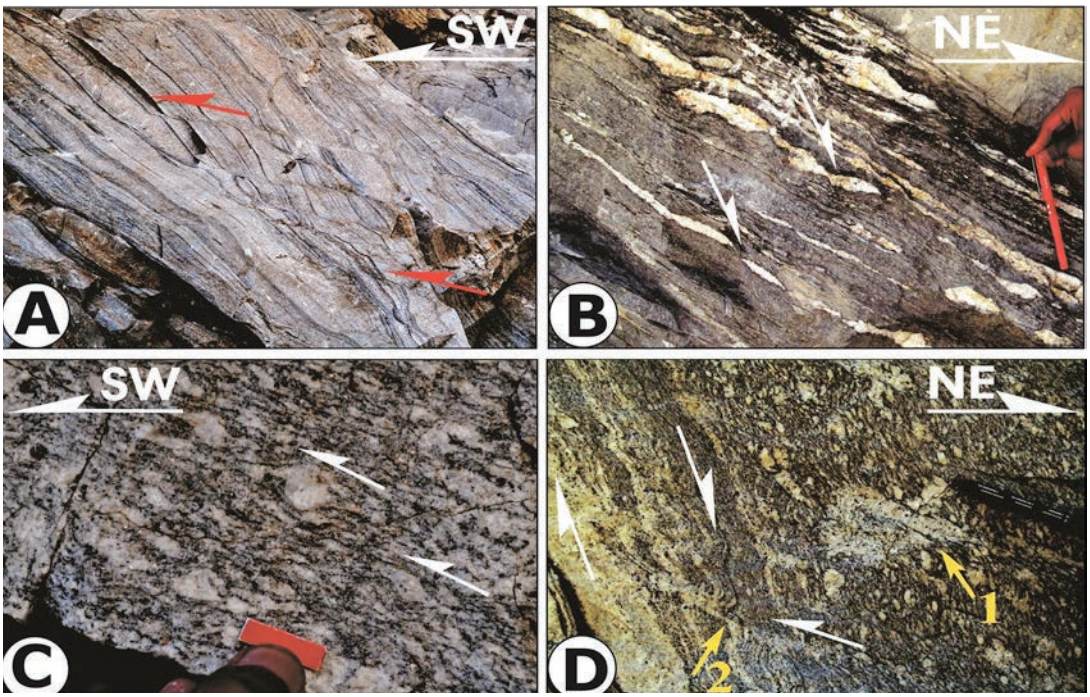

Figure 17
(A) Shear bands exhibiting top-to-the-SW upwards shearing in quartzo-feldsathicg gneiss and schist at Juma. (B) Steep shear bands with top-to-the-NE shear sense, displacing quartz boudins in gneiss at Juma. (C) First appearance of migmatite in the HHC at Stop 20 as porphyroblastic gneiss, showing top-to-the-SW shear sense. (D) Steeply-dipping stromatite migmatite folded by asymmetrical folds verging top-to-the-NE, shown by white arrows. Two new generations of melts observed along axial surfaces (arrow 2) and structureless patches (arrow 1).

cally inverted (Fig. 16B). Their deformation and flowage are remarkably developed in this zone, where cross-beds are even normal in disposition immediately before crossing Tamak stream. On the cliffs surrounding the village folding indicates large-scale overturning of the metamorphics.

Stop 20

Locality: Juma village. RM–92 (N 30°36'10":E 79°48'6")
Theme: First appearance of migmatite in the Bhapkund Formation of the HHC, and zone of shear sense reversal

Before approaching the very first exposure of migmatite in this section at Juma, a few locations between Tamak (Stop 19) and Juma (Stop 20) expose dark coloured psammitic gneiss and schist striking N315° and dipping about 35°NE with a strong mineral lineation plunging 300°/N350°. Immediately crossing Jumma Stream, one finds shear bands having both top-to-the-SW and top-to-the-NE geometries within few meters. Gently-dipping bands affect the gneiss-schist banding sigmoidally with thrust-type geometries (Fig. 17A), while vein quartz associated with psammite reveals normal shear sense with the hanging walls moving downwards (Fig. 17B).

True migmatite starts appearing at Stop 20 after crossing Juma where concordant leucosome and mesosomes alternate parallel to the main foliation with the former growing into quartz and feldspar porphyroblasts (Fig. 17C). These are deformed into asymmetrical megacrysts having their tails pointing a top-to-the-SW thrust geometry (Fig. 17C). At the same locality, steeply-dipping stromatite migmatite contains concordant leucosome sheets parallel to the main foliation of schist and are the first appearance of leucocratic melt within the HHC of this valley (Fig. 17D). These are folded into asymmetrical tight folds, having vergenge towards NE in contrast to other folds within the HHC. Interestingly, this outcrop also shows accumulation of new melt phases parallel to the moderately-dipping axial surfaces (towards NE) of these folds as well as into structuraless patches (See yellow arrows 1 and 2 in Fig. 17D).

Stop 21

Location: Before reaching Jelam village. RM–93 (N30°38'22":E79°49'45")
Theme: Folded and sheared stromatic migmatites

At this location, stromatic migmatite is folded into NE-verging asymmetrical close to isoclinal folds with enveloping surface striking N330° and dipping 600°NE (Fig. 18A). These are associated

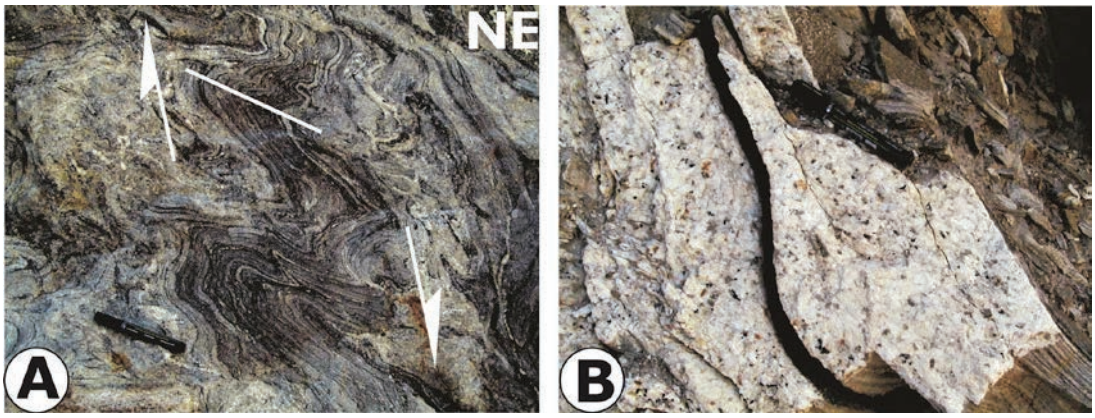

Figure 18
(A) Top-to-the NE downward verging train of folds and migmatitic characters at Stop 21. Scale: Marker pen. (B) Tourmaline-rich large discordant pegmatoidal vein cross-cutting the foliation. Scale: Marker pen. Loc.: About 200 m NE from Stop 21.

with sillimanite (fibrolite)-kyanite-garnet-biotite gneiss/schist, psammitic gneiss/schist. Further up from this location, concordant to discordant pegmatite veins, and small tourmaline-rich leucogranite lenses/dykes make their first appearence (Fig. 18B). Various stages of melt generation and their structural control in the Malari section have been documented by Jain et al. (2013), while this guide book will provide their stop-wise description later as these appear along the traverse.

Further one can also locate northerly-plunging open antiform at Jelam by observing northerly striking metamorphics on left bank of the Dhauli Ganga River.

At the microscale, stromatic migmatites show a spaced foliation made by the alternation of lepidoblastic layers of oriented biotite and sillimanite (mainly fibrolitic) and quartzo-feldspathic layers. Mineral assemblage is: biotite, quartz, plagioclase, K-feldspar, sillimanite, garnet and white mica with minor torumaline, zircon, apatite, opaque and monazite. Garnet is subhedral, often inclusion-rich (biotite, quartz, plagioclase), and sometimes has an atoll-like structure (Fig. 19A). It is worth to note that quartz inclusion in garnet and in K-feldspar are rounded or irregular, supporting the melt that was present in such rocks (Waters, 2001). Quartz and feldspar show evidence of dynamic recrystallization, such as lobate grain boundaries, windows and pinning microstructures. Quartz grains show well-developed chessboard extinction pattern (Fig. 19b) suggesting a high-temperature (≥ 650°C) deformation regime in these rocks (GBM II, Stipp et al., 2002a, b). White mica, present in low modal amount, could be subdivided in two different microstuctural groups: i) as larger anhedral grains with intergrowth/inclusion of sillimanite and minor feldspar, ii) as smaller euhedral grains, often cross cutting the fabric (Fig. 19c). The first type could be interpretated as relict of muscovite-involving melting reaction (schematic as muscovite + quartz + plagioclase = sillimanite + K-feldspar + melt), while the second type as a late (retrograde) white mica, forming on cooling/melt crystallization. More rarely, euhedral feldspar grains are observed in the quartz-feldspar domain (leucosome), again a microstructural support for the migmatic nature of these rocks (Fig. 19d).

Day 4: Jelam to Malari

We plan to cover mainly the upper formation of the HHC where the Bhapkund Formation has undergone extensive migmatization and produced leucogranite in various phases. We will also observe superposed ductile shearing in the HHC where an earlier top-to-the-SW contractional phase is superposed by younger extensional phase.

Stop 22

Locality: About 1 km before Bhapkund village. RM–95 (N30°39'51":79°50'50")
Theme: Syntectonically-grown porphyroblasts and migmatite

Intercalated stromatic migmatite, sillimanite-garnet-biotite-muscovite gneiss/schist and minor calc-silicate bands dip very steeply eastwards. As migmatite becomes pervasive between Stops 21 and 22, we have now entered into the Bhapkund Formation. Mantled porphyroblasts are characterized by reaction rims of mafic and feldspar-quartz mineral aggregates (melt?) surrounding garnet cores (Fig. 20A, see also insert), and are themselves bounded by the S-C foliation; these reveal top-to-the-SW upwards shear sense.

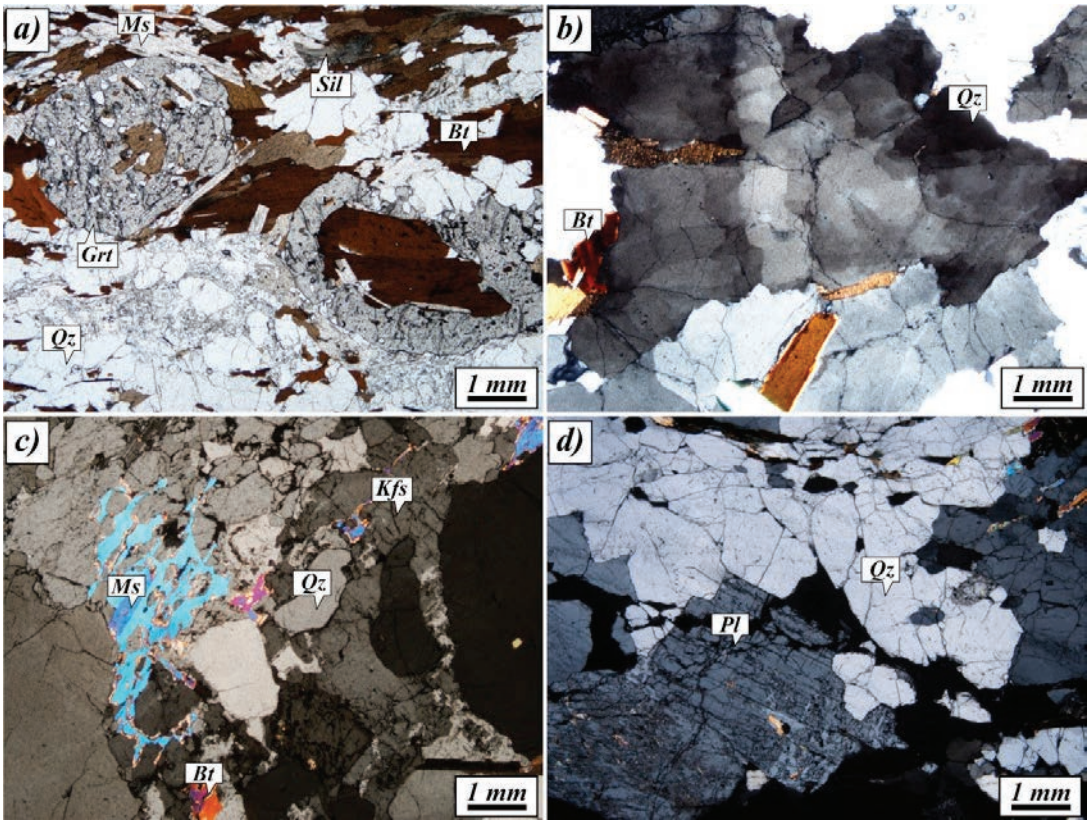

Figure 19
(A) Subhedral atollo-shaped garnet having biotite and quartz inclusions. (B) Anhedral quartz with chessboard extinction. (C) Sieved white mica porphyroblast. (D) Euhedral feldspar in a leucosome.

Stop 23

Locality: At Bhapkund village. RM–97/RM–21 (N 30°39'55":E 79°50'29")
Theme: Melt accumulation in extensional shear bands and necks of boudins.

As we travel through the upper parts of Bhapkund Formation, the lithology remains more or less same, i.e. sillimanite-garnet-biotite-muscovite gneiss/schist and migmatite. At Bhapkund, migmatite within the Formation is typically pervasive with alternating leucosome and mesosome, paralleling to the main foliation Sm (Fig. 20B). The foliations continued to dip in the N-NE direction. Some beautiful shear bands contain in situ biotite granite melts and dip steeply (50 to 60°) towards NE with the top-to-the-NE downward ductile shearing (Fig. 21). A foliation is distinctly visible in these bands, hence these are ductile in character. Interestingly, foliation boudins within the migmatite gneiss are marked by non-foliated leucogranite melt accumulation at their necks and appear to have generated during decompression melting without migration from the place of their generation (Fig. 21; see insert for details).

Stop 24

Locality: After crossing the Dhauli Ganga River on Bhapkund Bridge. RM–98/RM–7 (N30°40'00", E 79°50'30")
Theme: Deformed garnet, and superposed ductile shearing.

After crossing the Dhauli Ganga River on the Bhapkund Bridge, some rare garnet porphyroblasts are marked by filled 'V'-shaped gaping cracks, which are asymmetrically oriented and taper downwards (Fig. 22A). Individual larger grains still remain intact, but smaller fragment appears to have moved upwards, and provides indisputable evidence of top – to – SW (thrust) shear sense (Hippertt, 1993). Further along the main road, stromatite migmatite are isoclinally folded whose hinges are still preserved as rootless fold due to intense top-to-the-SW upwards ductile shearing (Fig. 22B). Interestingly, this ductile shearing is superposed by another but younger phase of top-to-the-NE downwards shearing (Fig. 22B).

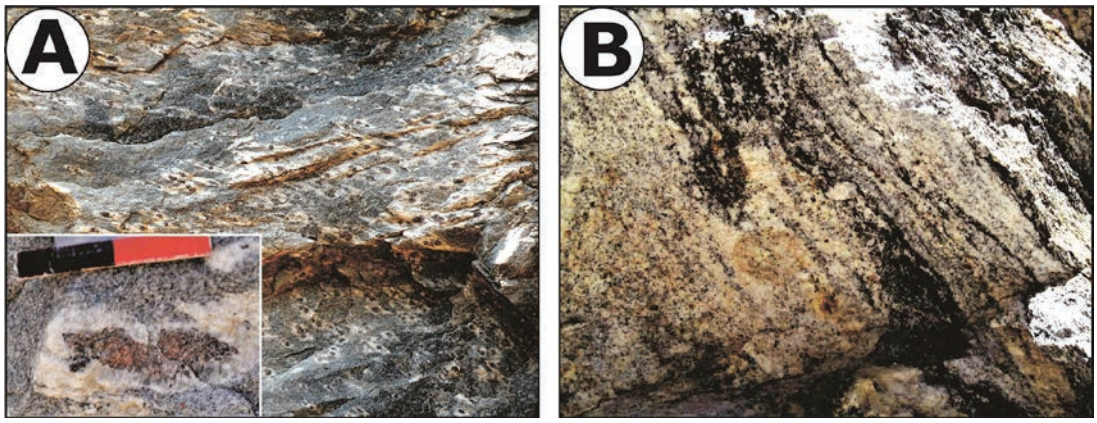

Figure 20
Characters of the Bhapkund Formation. (A) Mantled garnet porphyroblasts rimmed by biotite-rich mafics residues (melanosome), and quartz and plagioclase lucosome fraction developed around large garnets showing asymmetric melt stretching geometries (see insert) with top-to-the-SW-upwards shear sense. Stop. 22. Scale: Photograph width is about 8 cm. (B) Pervasive stromatite migmatite having leucosome and mesosome parallel to main foliation Sm.

Figure 21
Two-stage melt generation and their accumulation along steeply-dipping extensional shear bands and necks of extensional foliation boudins (insert). Stop 23.

Stop 25

Locality: Almost halfway between Bhapkund Bridge and opposite Kosa village on the main road. RM–99/RM–8 (N30°40'10":E 79°50'47")
Theme: Youngest leucogranite pods and veins

Main foliation within the fine-grained biotite-rich gneiss is overprinted by structureless small patches of leucogranite lacking and structural fabric (Fig. 23). Incipient melt has possibly generated along the main foliation and migrated into zones of least pressure for accumulation into pods.

Stop 26

Locality: On the main road opposite Kosa village. RM–100/RM–10 (N30°40'20": E79°51'24")
Theme: (i) Pegmatoidal granite along shear zone, and (ii) extensional shear zone.

Foliated and fine-grained biotite-rich gneiss is in-

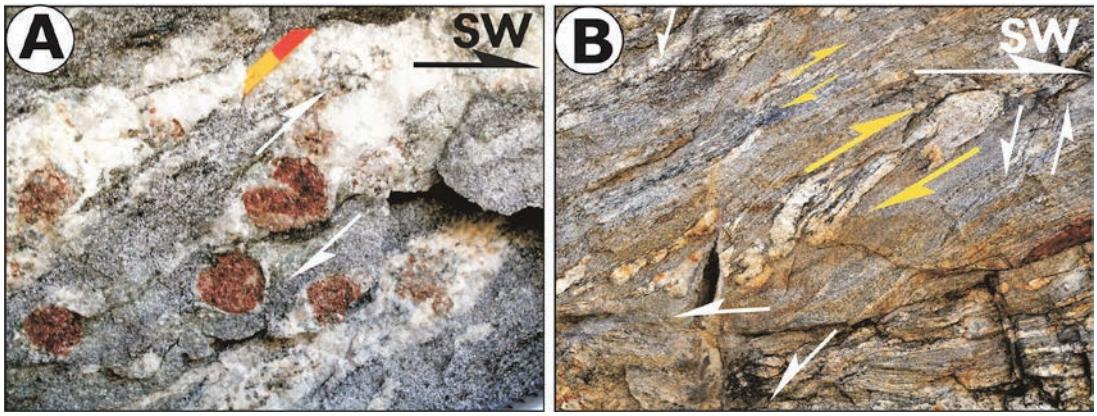

Figure 22
(A) 'V'-pull-apart in garnet from the HHC along the Dhauli Ganga Valley. Arrow points top-to-the-SW upwards. Stop 24. Scale: 2 cm. (B) Top-to-the-NE ductile shear bands superposed on rootless isoclinal folds, transposed along top-to-the-SW ductile shear zones. Stop 24. Scale: Length of photo ~2 m.

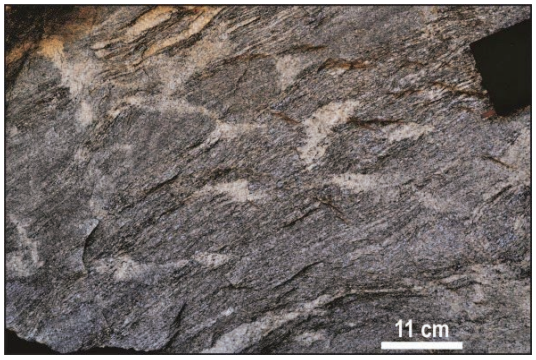

Figure 23
Structureless discordant and isolate leucogranite patches overprinting main foliation. Stop 25.

truded by undeformed tourmaline-bearing pegmatoidal granite along an extensional shear zone exhibiting top-to-the SW downward movement (Fig. 24A).

Within about 300 m distance from Stop 26 (RM–100), fine-grained biotite-rich gneiss is sigmoidally folded by a series of top-to-the-NE extensional shear zones which are smeared by thin plates of sillimanite layers and fibrolite needles (Fig. 24B). These zones strike almost NW and dip 45 to 50°NE. Top-to-the-NE downwards extension shear zones dominate in this area and are either sillimanite-bearing or intruded by granitic melt.

Stop 27

Locality: About 2 km before Malari on the main road. RM–105 (N 30°40'52":E79°53'30")
Theme: Typical mylonites associated with the South Tibetan Detachment System (STDS).

In this stop the high-grade rocks of the HHC are strongly overprinted by ductile shearing related to the STDS activity. At the outcrop scale well-developed mylonites with a top-to-the-North sense of shear can be observed (Fig. 25A) along with pods of sillimanite, pseudomorphosed on kyanite. At the microscopic scale these rocks have a spaced foliation with alternating granoblastic layers of quartz and plagioclase and biotite rich layers (Fig. 25B). Kyanite and garnet porphyroclasts are observed in such rocks, and is worth to note that sillimanite needles are aligned on the main foliation (Fig. 25B). Well-developed kinematic indicators such as kyanite fishes, C' shear bands also confirm the top-to-the north sense of shear affecting these rocks.

Day 5: Around Malari

This day is dedicated to the detailed study of the South Tibetan Detachment System (STDS) where its deformational imprints on the HHC and the Tethyan lithologies are clearly observed as both the ductile and brittle shear zones and related structures.

Stop 28

Locality: Malari village and adjoining areas. RM–28A: Above Kishanpur (N30°45'00": E79053' 13"). RM–28B/RM–14: On road (N30°42'32":E79°52'52"). RM–28C/RM–2: On road (N30°41'37":E79°53'00"). RM–28D/RM–A: On road (N30°41'00":E79°53'00"). RM– 28E: On road (N30°40' 57":79°53'45")
Theme: Investigating the South Tibetan Detachment System (STDS).

Moving towards Malari village just after crossing a small temple, one can see the Malari leucogranite. It is very narrow and unmappable on 1:50,000 scale and poorly exposed and mostly confined within the HHC. Though a few pegmatite bodies

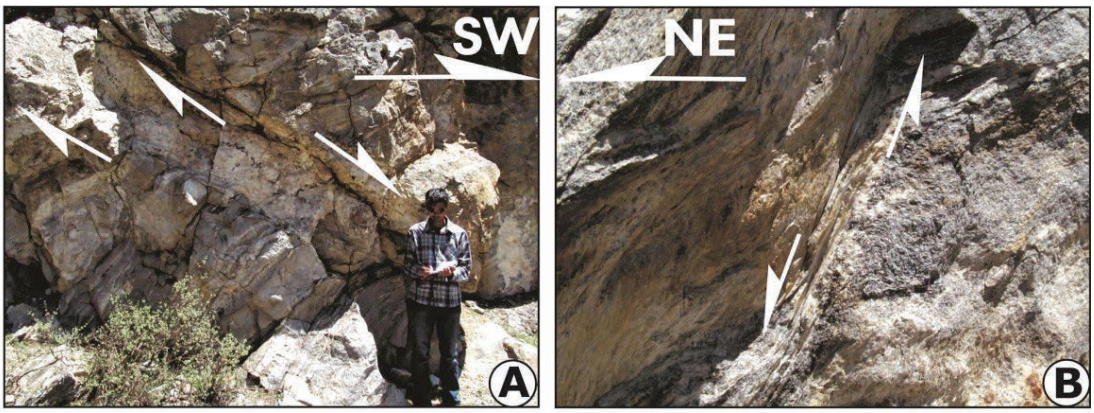

Figure 24
(A) SW-dipping tourmaline-bearing pegmatoidal granite along a shear zone. Stop. 26. (B) NE-dipping steep shear zones marked by well-developed sillimanite plates about 300 m from Stop 26 (Loc. RM–101).

are observed within the Martoli Formation near Niti village, most of these do not cut across the Martoli Formation (Jain et al., 2013).

First appearance of low grade Martoli rocks along the STD can be appreciated at the northern boundary of the Malari village. The STDS separates the low grade Martoli Formation of the THS from the high grade Bhapkund Formation of the HHC (Fig. 26). The Martoli Formation is constituted by low-grade quartzite and meta-arenite interbedded with metapelites. In the quarzitic layers, walking along the small river NE of the village, primary sedimentary structures, such as crossed bedding, are still recognizable (Fig. 27a). At the microscale a fine continuous foliation can be distinguished in the more pelitic levels associated to the dynamic recrystallization of illite (Fig. 27B). Undulatory extinction in quartz is predominant and the development of very small new grains could indicate a bulging recrystallization (BLG, Stipp et al., 2002a, b). Dynamic recrystallization is accompanied also by pressure solution mechanism that gives rise to brownish seams made by oxides and insoluble materials (Fig. 27B). Minor shape preferred orientation of detrital micas is present in the arenaceous levels.

From the Malari village, one can clearly see a nice view of the STDS contact (Fig. 28 A) separating the steeply-dipping HHC and the gentle THS (Figures 28A, B). After crossing the Malari village going further northwards, one can observe normal faults with their fault gouge zones with intense brittle fracturing and cataclasis in the HHC (Fig. 28C). These are the field evidences of extensional brittle deformation caused due to the STDS. As we can see from Figure 28D there is sharp change in lithology from highly deformed Bhapkund gneiss, the Malari Granite and the Martoli Formation. The STDS contact is not exposed at the Malari village. Many brittle faults dissect the Malari Granite, having subhorizontal geometry (Fig. 28E(i)) unlike the shear zones within the uppermost Bhapkund Formation. This has been possibly caused by the rollover antiformal disposition of the granite vis-à-vis the STDS.

Both type of shear sense indicators are observed within the Malari Granite. Fig. 28E(ii) shows the presence of older top-to-the SW upwards structures over which younger top-to-the NE downward structures are superimposed (right bottom of the Fig. 29E(ii)). But after crossing the Malari village while moving towards Ghamsali only top-to-the NE downwards structures were observed within the Martoli Formation (Fig. 28Eiii).

Ductile structures in the Malari Granite at the mesoscale are represented by S-C-C' fabric (Fig. 29A) and asymmetric feldspar porphyroclasts. At the microscale mica fishes, pointing to a top-to-the North sense of shear, are well developed. Mica fishes can be mainly referred to type I of Passchier and Trouw (2005) (Fig. 29B).

Quartz shows a bimodal distribution and a strong shape preferred orientation. Quartz presents undulatory extinction, subgrains (often very elongated) and new grains are commonly observed, suggesting a combination of bulging/subgrain rotation recrystallization mechanism, indicating a deformation temperature of c. 400-430°C (Stipp et al., 2002a, b). K-feldspar is fractured and show quartz recrystallization in the fractures (Fig. 29C). Tourmaline grains are often broken with fractures orthogonal to the mineral elongation, filled by quartz and blue tourmaline overgrowth on the former one. Brittle structures, such as transgranular fractures, superimposed on the ductile solid state deformation are observed, also at microscale in the Malari granite (Fig. 29D). Both macro and micro scale observations strongly disprove the previous conclusions of Sachan et al. (2010) regarding the Malari leucogranite like

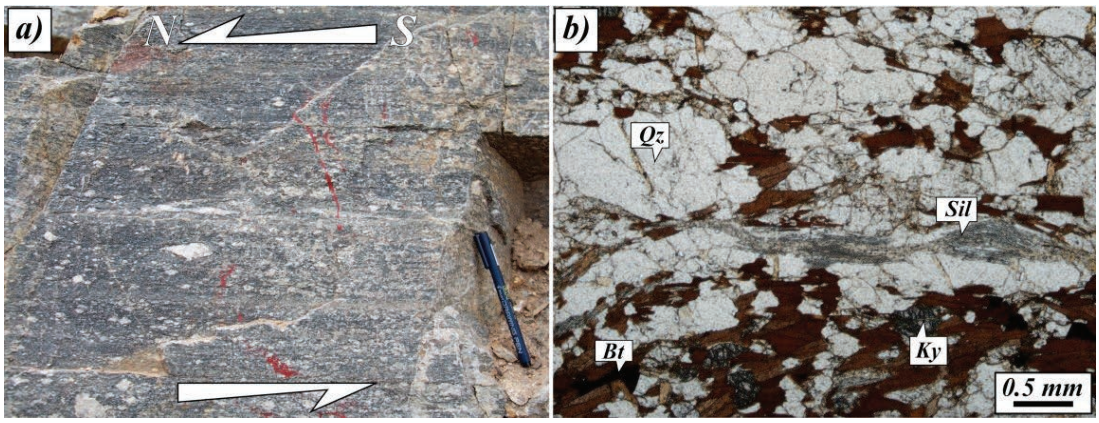

Figure 25
(A) Outcrop of the HHC gneiss strongly overprinted by STDS shearing. (B) Kyanite fish and sillimanite needles at the microscale.

a magmatic body cross-cutting the STDS, (in the Garhwal region) at c. 19 Ma. Up to now, the only undeformed granite clearly intruding both HHC and THS is the Bura Buri granite in Western Nepal (~ 24 Ma; Carosi et al., 2013).

Day 6: Malari – Niti

Last day of the traverse covers parts of the STDS along the strike towards NW between Malari and Niti village along the picturesque upper parts of the Dhauli Ganga Valley, where the uppermost parts of the HHC are exposed along this important tectonic boundary. One can observe different melt phases related to the leucogranite accumulation, superposed shear senses within uppermost parts of the HHC and deformation related to the STDS.
NOTE: GPS Locations beyond this point could NOT be recorded due to restrictions. Please refer the map (Fig. 1) for approximate location.

Stop 29

Locality: West of Kailashpur on the Malari-Niti Road. Loc. RM 15
Theme: The South Tibetan Detachment System (STDS), its deformation and stages of granite melts.

Further north from Malari and to the west of Kailashpur village, a few fresh cuttings on the road to Niti, the HHC metamorphics as grey paleosome are intimately interbanded with pervasive leucogranite neosomes; both having concordant foliation S1 (Fig. 30A). This is the indisputed evidence that the leucogranite started generating much earlier in the HHC, though the age of this phase of magma generation remains unconstrained. Within the nearby exposure, the HHC exhibits asymmetrical feldspar megacryst and is surrounded by S-C shear fabric; both exhibiting top-to-the-SW ductile shearing (Fig. 30B).

Stop 30

Locality: Between Ghamsali and Timarsain. RM–17
Theme: The HHC, its deformation and stages of granite melts

The Dhauli Ganga River flows through picturesque glacial valley till Bampa where an important tributary Amrit Ganga meets from the northwest. After the beautiful terrace at Ghamsali the Dhauli Ganga cuts a very steep gorge till Timarsain through sillimanite-bearing gneiss. Tight to isoclinal transposed F2 folds upon stromatic migmatite verging towards SW are affected by thrusts on limbs with their surfaces marked by new leucosomes (Fig. 31A). Top-to-the-SW ductile shear sense within 1.5 km of the STDS is decipherable from these folds and thrusts. However, within few meters, ductile shear zones having top-to-the-NE shearing are also encountered where both the leucogranite and the country rocks become foliated (Fig. 31B). Late stage cross-cutting undeformed, large and tourmaline-bearing leucogranite veins and apophyses manifest the terminal stage of the melt segregation and magmatic emplacement within the HHC.

Stop 31

Locality: Timarsain. RM–20
Theme: Ductile shearing due to the STDS
The Dhauli Ganga River cuts through almost vertical gorge between Ghamsali and Timarsain

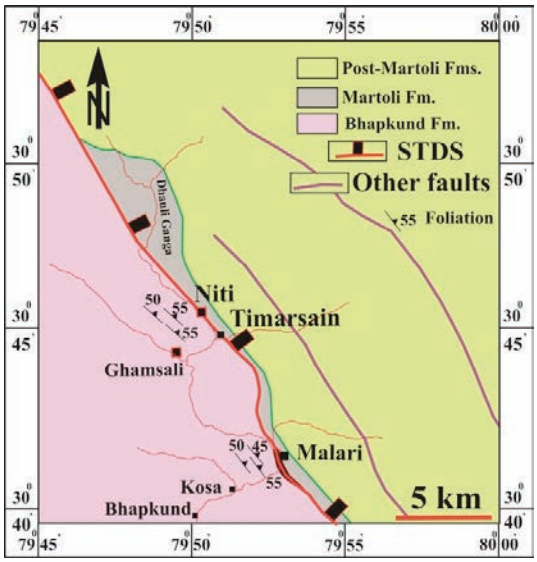

Figure 26
Simplified geological map of the Malari area separating the high grade HHC from the Tethyan Himalayan Series.

in the uppermost parts of the HHC. One of the best exposures of the deformation caused by the STDS is observed at Timarsain where the Dhauli Ganga River takes a L-shaped turn and opens up into the wide Niti valley after its junction with the Shalshal Nala. Megacrystic granite gneiss of the uppermost part of the HHC reveals an early top-to-the-SW shear sense from the asymmetrical feldspar (marked by red arrows), superposed by shear bands, S-C shear fabric and asymmetrical rotated feldspar indicating younger top-to-the-NE ductile shearing (Fig. 32B). Some of the fault surfaces are strongly striated to produce late-stage steeply-plunging lineation (Fig. 32D). While looking NW across the Dhauli Ganga River from the same locality one finds evidences of brittle to brittle-ductile superposed duplexes showing top-to-the NE shear sense along the STDS (Fig. 32C).

Stop 32

Locality: Beyond Niti village. RM–19
Theme: Tethyan Sedimentary Sequence and leucogranite

Further travelling along the road connecting Niti village, one starts observing exposures of the low grade metamorphosed Martoli Formation on the hanging wall of the STDS, where these muscovite-biotite schist and quartzite with detrital quartz grains are intruded by irregular and foliated leucogranite (Fig. 32A). The Martoli Formation strikes N300° and dips about 50° towards NE. These are cut by very steeply-dipping normal faults striking N-S dip of about 75° towards E. Our mapping reveals that the STDS runs parallel to the NW-SE trending Dhauli Ganga River between Timarsain and Niti village.

SUMMARY OF STRUCTURALLY-CONTROLLED MELT ACCUMULATION

Migmatite continued to be dominant in the upper parts of the HHC, where the Bhapkund Formation mainly contains these important rocks. Critical field observations highlight the following five stages of structurally-controlled melting and melt occurrences, Me1 to Me5 (Jain et al., 2013).

First Melt Stage (Me1): The earliest pervasive stage of melt occurrence is generally associated with the D1 deformation in the Bhapkund Formation. This stage has typically produced layered stromatic migmatite, parallel to the first visible and oldest foliation Sm within the country rocks (Figs. 20B; 30A). New leucosome imperceptibly grades and permeates the mesocratic grey paleosome of the host gneiss/schist, having large decimeter thick foliated leucogranite, as well. The most obvious feature of Me1 generated melt is the presence of a strong foliation within leucosome and parallelism with the strong tectonic foliation (Fig. 30A).

Second melt stage (Me2): Stromatic migmatite has undergone very strong SW-verging asymmetrical and nearly-isoclinal folding during the D2 event, which has transposed the Sm foliation into new S2 foliation, when highly-strained limbs are attenuated and thrust towards SW along ductile shear zones. Many of these limbs and shear zones are now occupied by very thin smear of new leucogranite during the Me2 stage of melt generation and accumulation (Fig. 31A). As the leucosomes of the Me1 stage becomes thicker in the fold hinges, considerable flowage took place from the attenuated limbs into hinges. Possibly, the melt has also flown along the thrusts, bounding the limbs during this stage (Fig. 31A).

Third Melt Stage (Me3): The uppermost amphibolite-facies and sillimanite bearing gneiss exhibits discrete normal-sense shear bands to the south of Malari where earlier foliation Sm has developed SW- and NE- dipping ductile shear bands, now occupied by thin leucosomes (Figs. 21; 31B). These bands die out within the main foliation and thus, define the extensional flanking structures. Both the conjugate set reveal an episode of layer-parallel extension, possibly related to

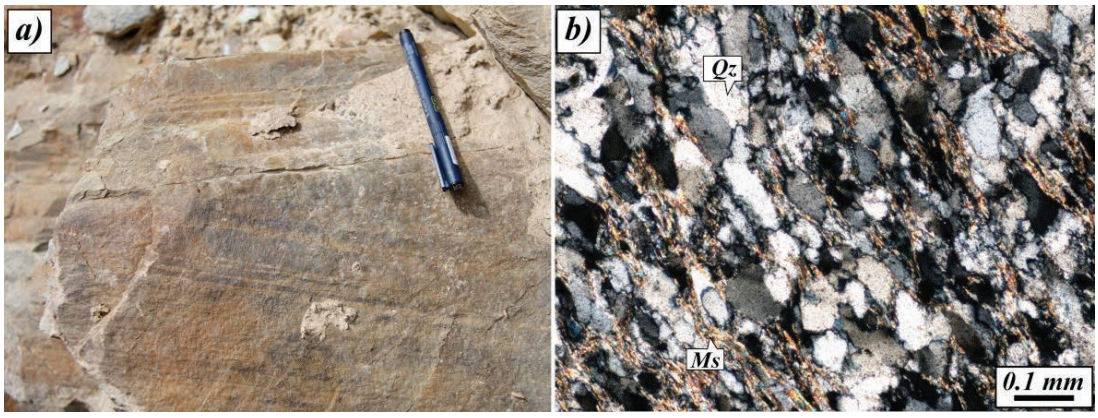

Figure 27
(A) Cross-bending lamination in quartzite of the Martoli formation. (B) Microscopic aspect of quartzite form the Martoli Formation showing a prominent S1 continuous foliation.

the movements along the STDS.

In addition, a late stage layer-parallel extension has produced extensional foliation boudins whose necks are now occupied by structureless leucosome (Fig. 21). The Sm foliation within the melanosome swings into the neck both ways and is deformed around neck of the boudins where newly-developed leucosome occupies sites of decompressed necks. In contrast to the leucosome of the shear bands, this new leucosome within the necks remains structureless and appears to have developed late during decompressional melting of the HHC.

Fourth Melt Stage (Me4): This stage of melt formation basically incorporates veins and veinlets across the earlier fabric (D1) and is developed mainly on the Me1 stage stromatite (Figs. 31C, D). Tourmaline-rich ataxial leucocratic pegmatite extensional veins are structureless where quartz, feldspar and tourmaline fill in the cavities. Dilatant veins are seen intruding Me1 layers and surround them completely with breccia-like agmatitic appearance.

Fifth Melt Stage (Me5): This is the last stage of melt formation where melt has accumulated as structureless net-like patches on the foliation Sm, which is totally destroyed in the region now occupied by these patches (Fig. 23).

OBSERVATIONS

Though top-to-SW shear sense indicators are very common within the HHC, kinematic indicators having only the top – to – SW shear sense are observed within the Munsiari and Joshimath Formations and continue till the upper parts of the Suraithota Formation. Structures showing top – to – NE shear sense first start appearing in the middle parts of the Suraithota Formation somewhere between Suraithota and Tamak at Location I (N30°34'12": E79°44'56") (Fig. 33). However, shear structures showing the top – to – SW structures remain the dominant shear fabric and are prominent up to Tamak village. Between Tamak (Location II - N30°35'49":E79°47'31") and the next village Juma, the zone contains many folds and flow structures along with the first appearance of leucogranites. However, shear sense indicators are absent throughout this narrow zone. After crossing Juma (Location III – N30°36'7":E79°48'18"), kinematic indicators with top – to – NE shear sense become dominant with the first appearance of migmatite. A large migmatite zone is observed after crossing the next village Jelam. The migmatites are ubiquitously distributed up to Malari but they are observed to be dominant only in the upper parts of the Bhapkund Formation. A few relict structures of top – to – SW shear sense are also observed along with the dominant top – to – NE shear fabric between Bhapkund and Malari. Beyond Malari (Location IV - N30°40'52":E79°53'20"), i.e. in the Martoli Formation, we observed exclusively top – to – NE downward shear sense indicators.

On the basis of our field observations and analysis of the shear sense indicators, the whole HHC has been subdivided into the following five structural zones between Helang and Ghamsali – Niti, including parts of the LHS and the THS (Fig. 33). The above classification is based on our shear sense analysis and the simple fact that older phase ductile shear fabric (DS1) or the top – to – SW shear sense indicators represents a compressional/contractional environment, while the younger ductile shear phase fabric (DS2) or the top – to – NE shear sense indicators represent an extensional environment. These zones have been mapped as A to E in Figure 33, while observational points of

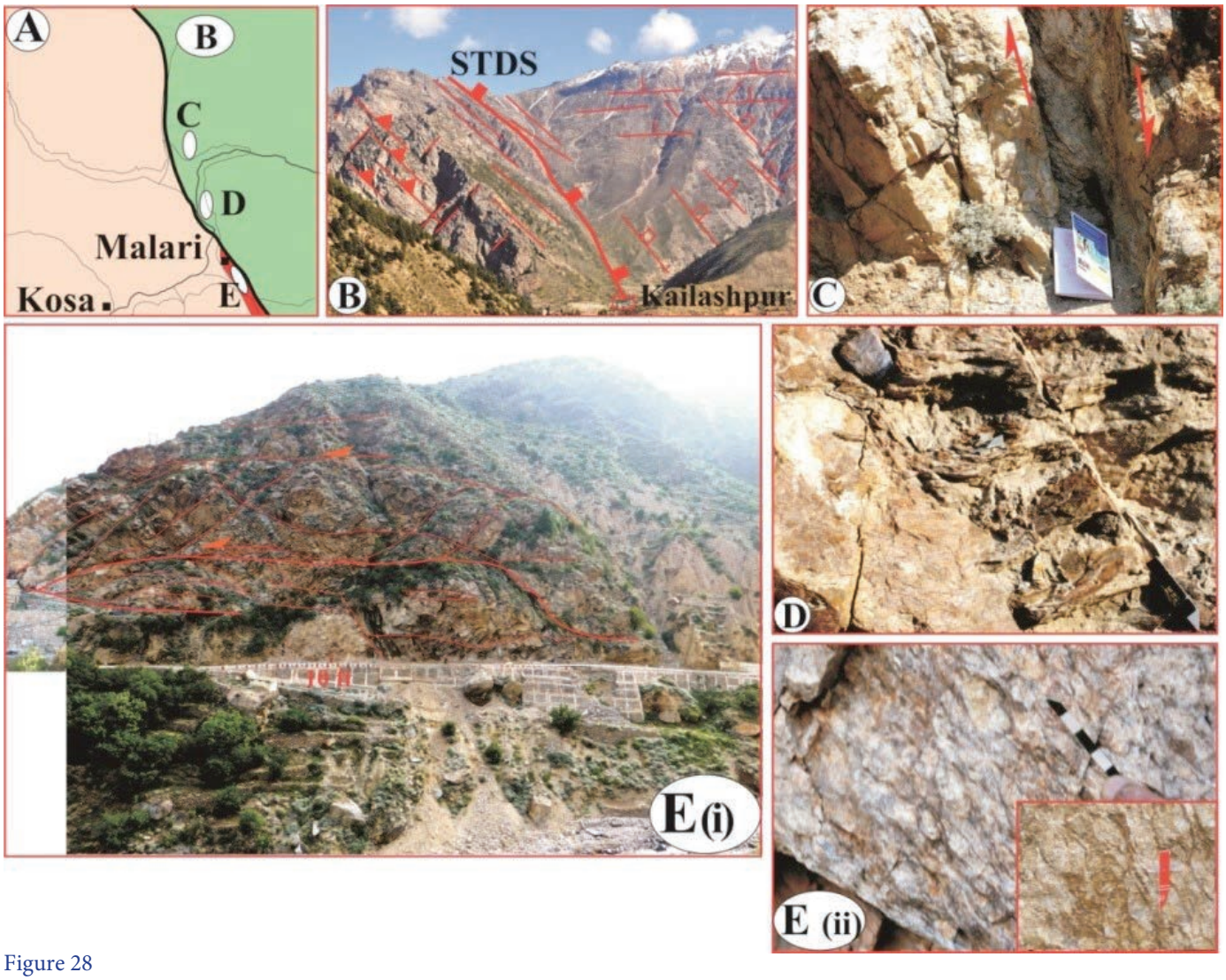

Figure 28
(A) Local geological map of the STDS showing various structures close to Malari village. (B) The STDS above Kailashpur, observed from Malari. Steeply-dipping HHC gneiss (left) is tectonically overlain by gently-dipping Martoli Formation. Unfilled rectangles indicate small-scale faults. Dash lines are traces of joints. (C) Normal fault and its fault gouge and breccia within leucogranite due to isolated splay extensional fault of the STDS. About 4 km from Malari on the Malari-Niti road. (D) The Martoli quartzite deformed by brittle-ductile extensional fault zone E ii near Malari. Scale – Pen. (E i), Overall fracture E iii pattern in deformed granite with thrusts, normal faults and joints at Malari village. Loc. (E ii), Insert shows details of subhorizontal thrust. (E iii) Porphyroclastic Malari granite with asymmetrical megacrysts having top – to – SW (arrow) overthrust sense, and shear bands with top – to – NE downward shear sense on the road near the village Malari, thus indication of the presence of both relict and younger kinematic indicators. Scale: 5 cm.

their changes in the field are indicated as I to IV.

(A) Pure contractional zone (PCZ), exhibiting only the DS1 top – to – SW shear phase fabric.

(B) Dominant contractional zone (DCZ), DS2 movement planes with top – to – NE shear sense make their first appearance, but the DS1 fabric remains dominant.

(C) Transition zone (TZ) having no DS1 and DS2 shear sense indicators, but is marked by considerable rock flowage.

(D) Dominant extensional zone (DEZ), in which the DS2 phase shear fabric is dominant over the DS1 phase shear fabric, and

(E) Extensional zone (EZ) with only the DS2 phase shear fabric within the THS.

According to the above classification, the PCZ is the zone from the upper parts of the LHS up to the middle parts of the Suraithota Formation; DCZ is the zone accommodating the upper parts of Suraithota Formation up to the village Tamak. This zone extends up to approximately 18 km

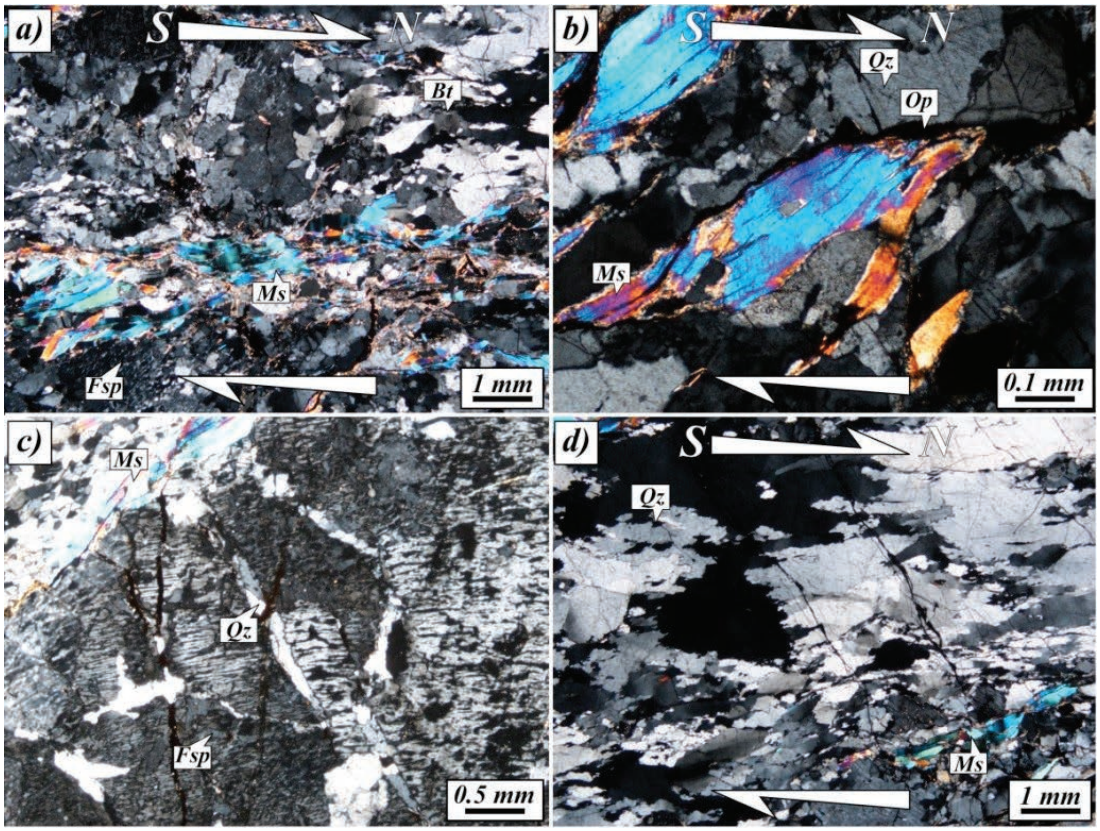

Figure 29
(A) Deformed Malari leucogranite. (B) Details of white mica fish pointing a top-to-the North sense of shear. (C) Quartz filled fractures in feldspar. Note also late intergranular fractures. (D) Dynamic recrystallization of quartz. Note the late intergranular fractures.

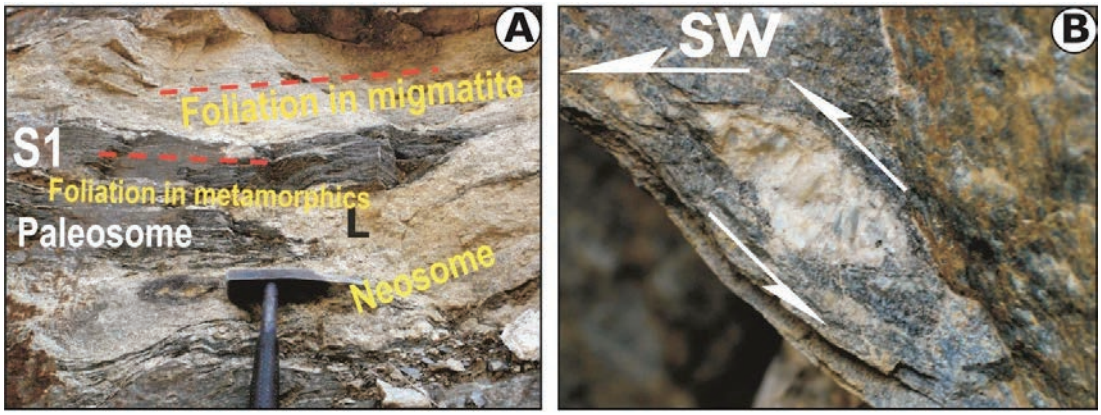

Figure 30
(A) Pervasive and concordant paleosome and neosomes within the upper parts of the HHC at Stop 29. Note parallel foliation S1 in metamorphics and foliated leucogranite. (B) Asymmetrical σ-shaped feldspar porphyroclast surrounded by S-C shear fabric.

(map distance) from the Vaikrita Thrust (VT); TZ is the zone between the villages Tamak and Juma. It starts at a distance of 18 km approximately from the VT and is around 2 km wide; is the zone starting after the village Juma up to Malari. This zone accommodates upper parts of the Suraithota Formation and the entire Bhapkund Formation. It starts at a distance of 20 km from the VT; EZ is the zone which accommodates the entire Martoli Formation and starts at a distance of about 30 km from the VT (Fig. 33).

Observation of numerous shear sense indicators along these valleys revealed two phases DS1 and DS2 of ductile shear deformation. The later phase DS2 showing top – to – NE downward shear sense was superposed over the older phase DS1 showing top – to – SW upward shear sense. The DS1 indicates that the HHC has been deformed within a broad non-coaxial ductile shear zone of the overthrust type with a consistent top – to – SW sense of movement. It also suggests an early deformation history of the HHC involving large scale SW – directed ductile shearing within the HHC belt, associated with the India – Asia continental convergence and compressional tectonics (Jain and Manickavasagam, 1993; Patel et

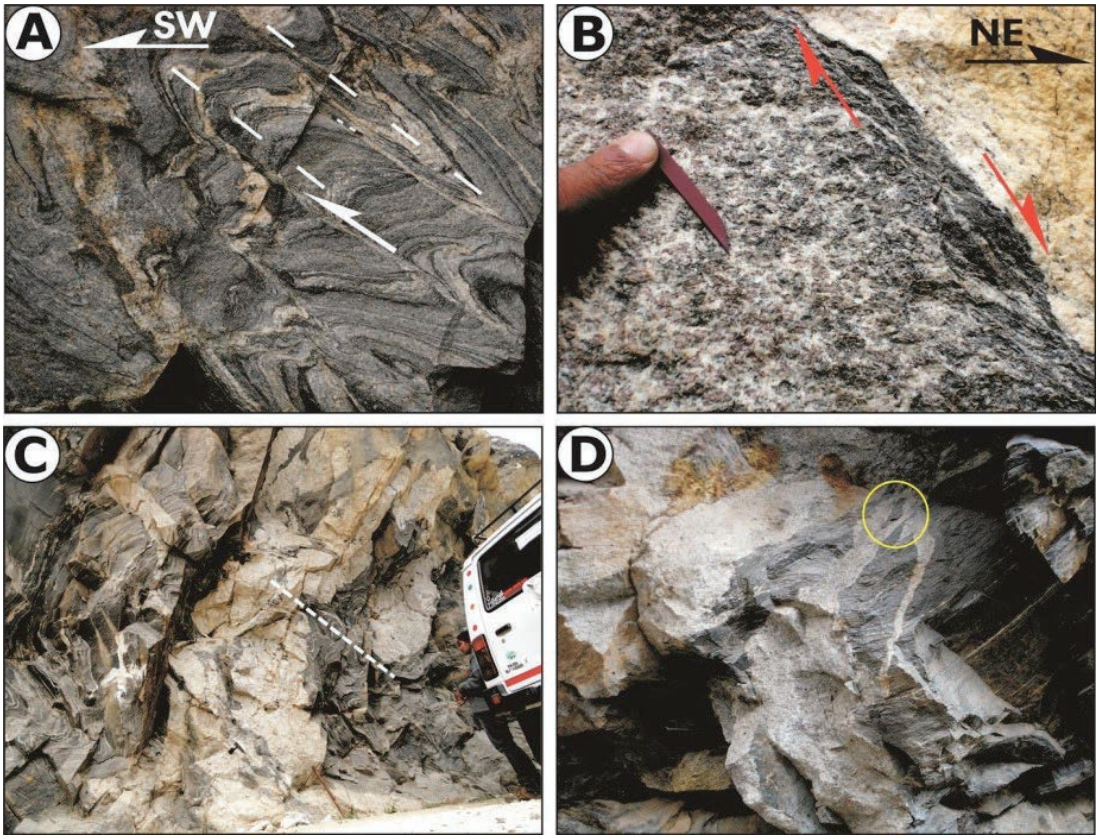

Figure 31
(A) SW-verging thrusts and isoclinal folds of stromatic migmatite. Note new leucosome along thrusts. (B) NE-shear sense from normal ductile shear zone having new shear fabric. (C) Cross-cutting leucogranite veins across F2 folds in HHC metamorphics. (D) Leucogranite apophyses from main vein and development of xenoliths.

al., 1993). Though it is difficult to envisage precise relationship between the ductile shearing within the HHC and its movement along the MCT, it is likely that the latter represents a zone of very high ductile strain. The STDS, on the contrary, is associated with extensional deformation.

The present work highlights the distribution pattern of various kinematic indicators along the Alaknanda – Dhauli Ganga section and is useful in understanding the evolution of the Himalayan metamorphics within a framework of various recent tectonic models like (i) ductile shearing (Jain and Manickavasagam, 1993), (ii) channel flow (Beaumont et al., 2001, 2006) and (iii) critical wedge/extrusion (Grasemann, et al., 1999; Webb et al., 2007). The ductile shear model postulates consistent top – to – SW thrust shear sense from various kinematic indicators within a broad ductile shear zone, the HHC belt, where mm- to dm-scale ductile shearing along S-C shear fabric caused the inverted metamorphism and decompression melting in the upper parts (Jain and Manickavasagam, 1993); top – to – NE shear sense near its upper margin remained not so well explained. The channel flow model and its different variants visualizes either (i) a pure Couette (or linear) flow between rigid plates where these move relative to one another and produce uniform simple shear across the channel, (ii) a pure Poiseuille (or parabolic) flow between stationary rigid plates where horizontal gradients in lithostatic pressure and frictional resistance along channel boundaries produce greatest velocities in its center with decreasing velocities toward the margins, leading to development of opposing shear senses, or (iii) a combination of the two (Grujic, 2006; Godin et al., 2006 and references therein; Langille et al., 2010). The critical wedge/extrusion models postulate southward extruding metamorphic belt, bounded by the MCT and the STDS at the base and the top, respectively (Burchfiel et al., 1992; Langille et al., 2010).

Shear sense indicators from the HHC belt of the Alaknanda and Dhauli Ganga Valleys could be explained by a combination of the pure Couette (or linear) flow and pure Poiseuille (or parabolic) flow within either a ductile shear zone or a channel, bounded by the MCT and the STDS where top – to – SW shear indicators are superposed by the top – to – NE directed structures over a wide zone near the STDS, assuming a contemporaneous activity of the MCT and STDS. The Couette (or linear) flow possibly provided top – to – SW shearing throughout the shear zone/channel to

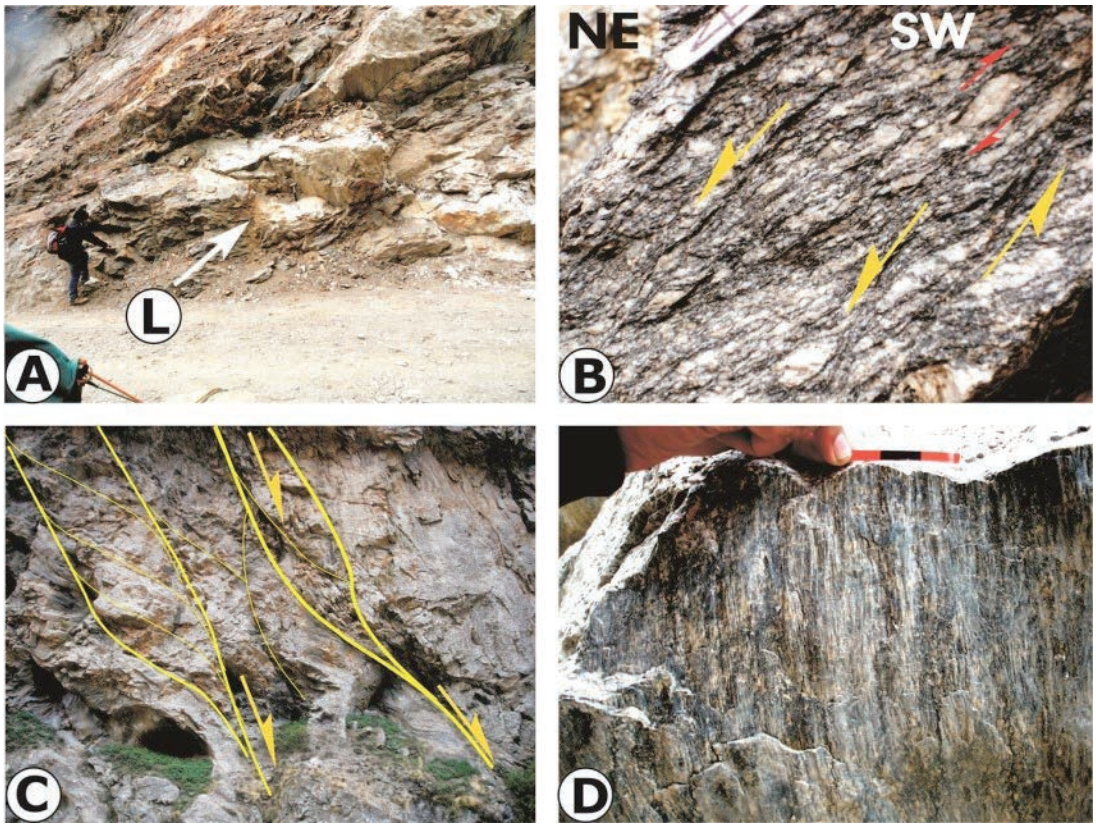

Figure 32
(A) Muscovite-biotite schist and quartzite of the Martoli Formation on the hanging wall of the STDS intruded by irregular and foliated leucogranite. Stop- Above Niti village. Scale: Hammer. (B) Megacrystic granite gneiss of the uppermost part of the HHC showing both top-to-the-SW asymmetrical feldspar, superposed by shear bands, S-C shear fabric and asymmetrical feldspar indicating top-to-the-NE ductile shearing. Location: RM–20. (C) Steep NE-dipping brittle-ductile shear zones causing development of normal duplexes paralleling the STDS. On opposite hill face of Timarsain. Location: RM–20A. Scale: Photo about 10 m. (D) Striations along a fault showing thrust geometry at Timarsain. Location: RM–20. Scale 3 cm.

start with, and was subsequently superposed by the Poiseuille (or parabolic) flow at a later stage; both the flows would remain indistinguishable from each other in the lower parts of the shear zone/channel. It is only after crossing the Transition Zone that the structures of the Poiseuille flow will start showing in the shear zone/channel due to their opposite vergence. However in Western Nepal, the contemporaneous activity of MCT and STDS has beeen discussed by Carosi et al. (2013) and Montomoli et al. (2013). Moreover, Montomoli et al. (2013) demonstrated that ductile shearing within the HHC was not contemporaneous but becomes younger from north to south, where it is localized along discrete shear zones.

CONCLUSIONS

Various small-scale ductile to brittle shear structures such as S-C and S-C' shear fabric, porphyroclasts and porphyroblasts, mineral fish, asymmetric boudins, duplex and shear zones have been used for deciphering the shear sense within the Higher Himalayan Crystallines along the Alaknanda and Dhauli Ganga Valleys of the Uttarakhand Himalaya. This analysis revealed crucial information regarding two phases of ductile shear deformation, the DS1 and DS2, where the DS1 is the older phase of SW-verging shearing associated with the compressional tectonics and the DS2 is the younger phase of late orogenic NE-verging normal faulting/shearing. On close examination of these structures, five distinct zones have been mapped in this section: (i) pure compressional zone (PCZ) with only the DS1 shear fabric, (ii) dominant compressional zone (DCZ) with DS1 fabric dominating over the DS2 phase, (iii) transition zone (TZ) with extensive flowage having no shear sense indicators, (iv) dominant extensional zone (DEZ) with more frequent DS2 phase structures over the DS1 phase, and (v) pure extensional zone (EZ) having only the DS2 phase within the THS. The NE-directed extensional ductile shearing is distributed for nearly 20 km wide zone in the Dhauli Ganga Valley. The STDS shear fabric appears to be highly localized in character. These fabric/kinematic indicators become useful tools in critically assessing various tectonic models like ductile shear, critical wedge and channel flow models for the evolution of this part of the Himalaya, though quantitative work on strain, metamorphic gradients and geochronology is required to precisely select the model for evolution of the

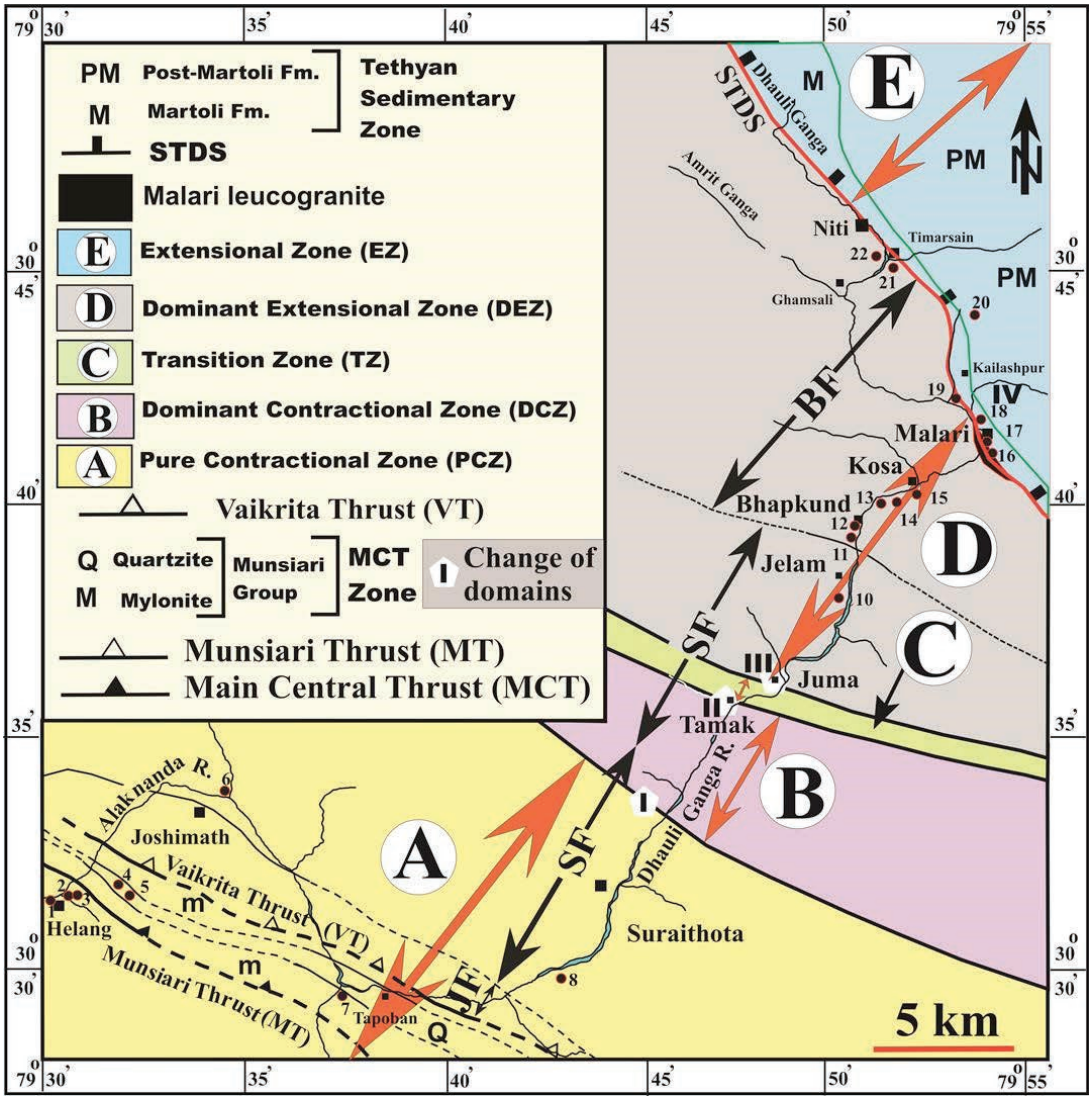

Figure 33
Geological map of the Alaknanda and Dhauli Ganga Valleys showing distribution of contractional DS1and extensional DS2 phases of shear structures and their transitions (red arrows) on the basis of shear sense analysis, Uttarakhand Himalaya. Black arrows represent lithological boundaries within the Vaikrita Group. JF – Joshimath Formation. SF – Suraithota Formation. BF – Bhapkund Formation. Note domain boundaries of the DS1and DS2 shear structures and their transitions transgress the lithological boundaries. Change of domains indicated by I to IV. Locations of photographs used in this paper are also shown.

HHC. A possible model for the evolution of this part of the Himalaya is therefore either a ductile shear zone in which an older SW-verging ductile shearing associated with the compressional tectonics (the Couette flow) is superposed by the younger DS2 late orogenic NE-verging normal faulting/shearing phase as a consequence of the Poiseuille flow. Another possibility to explain the described kinematics is the critical taper model proposed by Kohn (2008) in which contractional and extensional shearing act in response of the chaning dynamic of the orogenic wedge. Only after a precise geochronology of the shear zone it is possible to fully discriminate among the proposed models.

ACKNOWLEDGEMENTS

The authors acknowledge the Editors for inviting us to contribute to the Special volume on the Geological Field Trips in the Himalaya, Karakoram and Tibet of the Journal of Virtual Explorer. This paper has emerged out from integrated geological studies across a typical cross-section through the Higher Himalaya as a part of M. Tech. thesis by MS, PS and LK for the Head, Department of Earth Sciences, IIT Roorkee is thanked for providing the facilities. MS and RS also thank the Indian Academy of Sciences (IAS), Bangalore for the award of the Summer Fellowship. AKJ is thankful to the Indian National Science Academy (INSA) for the Senior Scientist Scheme and Prof. S.K. Bhattacharyya, Director, CSIR-Central Building Research Institute (CBRI), Roorkee for necessary facilities. P. K. Mukherjee acknowledges the Director, Wadia Institute of Himalayan Geology Dehra Dun for the facilities and the financial support. Research and field trip in Garwhal was supported by MIUR, PRIN 2010-2011 project and funds

from Pisa and Torino Univerisites for R. Carosi, C. Montomoli and S. Iaccarino.

REFERENCES

Academia Sinica, 1979. Geological map of Lhasa-Nyalam area, Xizang (Tibet), 1:1500.000. In A Scientific Guidebook to South Xizang (Tibet). Academia Sinica, Beijing.

Ahmad, T., Harris, N., Bickle, M., Chapman, H., Bunbury, J. and Prince, C., 2000. Isotopic constraints on the structural relationships between the Lesser Himalayan Series and the High Himalayan Crystalline Series, Garhwal Himalaya. Geological Society of America Bulletin, 112 (3), 467–477.

Beaumont, C., Jamieson, R. A., Nguyen, M. H. and Lee, B., 2001. Himalayan tectonics explained by extrusion of a low-viscosity crustal channel coupled to focused surface denudation. Nature, 414, 738–742.

Beaumont, C., Nguyen, M., Jamieson, R. and Ellis, S., 2006. Crustal flow models in large hot orogens. In Channel Flow, Ductile Extrusion and Exhumation in Continental Collision Zones (eds. Law, R.D., Searle, M.P., Godin, L.), Geological Society, London, Special Publications, 268, p. 91–146.

Burchfiel, B. C., Chen, Z., Hodges, K. V., Liu, Y., Royden, L. H., Geng, C. and Xu, J., 1992. The South Tibetan Detachment System Himalayan orogen: extension contemporaneceous with and parallel to shortening in a collisional mountain belt. Geological Society of America (Special Paper), 269, 1-41.

Burchfiel, B.C. and Royden, L.H., 1985. North-south extension within the convergent Himalayan region. Geology, 13, 679-682.

Burg, J.P., 1983. Tectogénèse comparée de deux segments de chanes de collision: le sud du Tibet et la Chane Hercynienne d'Europe. Thèse d'Etat, Universite 'des Sciences et Techniques du Languedoc, Montpellier, 361 pp.

Burg, J.P., Brunel, M., Gapais, D., Chen, G. M. and Liu, G.H., 1984. Deformation of leucogranites of the crystalline Main Central thrust sheet in southern Tibet (China). Journal of Structural Geology, 6, 535–542.

Caby, R., Pêcher, A. and Le Fort, P., 1983. Le grand chevauchement central himalayen: Nouvelles données sur le métamorphisme inverse à la base de la Dalle du Tibet. Revue de Géologie Dynamique et de Géographie Physique, 24, 89–100.

Carosi, R., Lombardo, B., Molli, G., Musumeci, G. and Pertusati, P.C., 1998. The South Tibetan Detachment System in the Rongbuk valley, Everest region. Deformation features and geological implications. Journal of Asian Earth Sciences, 16, 299–311.

Carosi, R., Montomoli, C., Rubatto, D., and Visonà D., 2013. Leucogranite intruding the South Tibetan Detachment in western Nepal: implications for exhumation models in the Himalayas. Terra Nova, 25, 478-489, (doi:0.1111/ter.12062).

Célérier, J., Harrison, T.M., Webb, A.A.G., and Yin, A., 2009. The Kumaun and Garwhal Lesser Himalaya, India; Part 1, Structure and stratigraphy. Geological Society of America Bulletin, 121, 1262–1280. doi:10.1130/B26344.1.

Davidson, C., Grujic, D.E., Hollister, L.S., and Schmid, S.M., 1997, Metamorphic reactions related to decompression and synkinematic intrusion of leucogranite, High Himalayan Crystallines, Bhutan: Journal of Metamorphic Geology, 15, 593–612.

Dézes, P.J., Vannay, J.C., Steck, A. , Bussy, F. and Cosca. M., 1999. Synorogenic extension: Quantitative constraints on the age and displacement of the Zanskar shear zone (northwest Himalaya). Geological Society of America Bulletin, 111(3), 364–374.

Gansser, A., 1964. Geology of the Himalayas. London/New York/Sydney: Wiley Interscience. 289 p.

Godin, L., Grujic, D., Law, R.D. and Searle, M.P., 2006. Channel flow, ductile extrusion and exhumation in continental collision zones; an introduction. In Channel Flow, Ductile Extrusion and Exhumation in Continental Collision Zones (eds. Law, R.D., Searle, M.P., Godin, L.), Geological Society, London, Special Publications, 268, 1–23.

Grasemann, B., Fritz, H. and Vannay, J.C., 1999. Quantitative kinematic flow analysis from the Main Central Thrust Zone (NW-Himalaya, India): implications for a decelerating strain path and the extrusion of orogenic wedges. Journal of Structural Geology, 21, 837–853.

Grujic, D., 2006. Channel flow and continental collision tectonics: an overview. In Channel Flow, Ductile Extrusion and Exhumation in Continental Collision Zones. (eds Law, R.D., Searle, M.P., Godin, L.). Geological Society,

London, Special Publications, 268, 25–37.
Grujic, D., Casey, M., Davidson, C., Hollister, L.S., Kundig, R., Pavlis, T. and Schmid, S., 1996. Ductile extrusion of the Higher Himalayan Crystalline in Bhutan: Evidence from quartz microfabrics. Tectonophysics, 260, 21–43.
Grujic, D., Hollister, L.S., Parrish, R.R., 2002. Himalayan metamorphic sequence as an orogenic channel: insight from Bhutan. Earth and Planetary Science Letters, 198, 177–191.
Gururajan, N.S. and Choudhuri, B.K., 1999. Ductile Thrusting, metamorphism and Normal faulting in Dhauliganga Valley, Garhwal Himalaya. Himalayan Geology, 20(2), 19–29.
Heim, A. and Gansser, A., 1939. Central Himalaya: geological observations of the Swiss expedition 1936. Memoir Society Helvetica Science Nature 73, 1–245.
Herren, E., 1987. Zanskar shear zone: Northeast-southwest extension within the Himalayas (Ladakh, India). Geology, 15, 409–413.
Hippertt, J.F.M., 1993. 'V'-pull-apart microstructures: a new shear-sense indicator. Journal of Structural Geology, 15, 1393–1403.
Hodges, K.V., Parrish, R.R. and Searle, M.P., 1996. Tectonic evolution of the central Annapurna Range, Nepalese Himalayas. Tectonics, 15, 1264–1291.
Hodges, K.V., 2000. Tectonics of the Himalaya and southern Tibet from two perspectives. Geological Society of America Bulletin, 112(3), 324–350.
Hubbard, M.S., 1996. Ductile shear as a cause of inverted metamorphism: Example from the Nepal Himalaya. Journal of Geology, 104, 493–499.
Jain, A.K., 2014. When did India–Asia collide and make the Himalaya? Current Science, 106, 254–266.
Jain, A.K. and Manickavasagam, R.M., 1993. Inverted metamorphism in the intracontinental ductile shear zone during Himalayan collision tectonics. Geology, 21, 407–410.
Jain, A.K. and Patel, R.C., 1999. Structure of the Higher Himalayan Crystallines along the Suru-Doda valleys (Zanskar),NW Himalaya. In Geodynamics of the NW Himalaya (eds. Jain, A.K. and Manickavasagam, R.M.), Gondwana Research Group Memoir, 6, 91–110.
Jain, A.K., Manickavasagam, R.M., and Singh, S., 1999. Collision tectonics in the NW Himalaya: Deformation, metamorphism, emplacement of leucogranite along Beas-Parbati Valleys, Himachal Pradesh. Gondwana Research Group Memoir, 6, 3–37.
Jain, A.K., Seth, P., Shreshtha, M., Mukherjee, P.K. and Singh, K., 2013. Structurally-controlled melt accumulation: Himalayan migmatites and related deformation, Dhauli Ganga Valley, Garhwal Himalaya. Journal of the Geological Society of India, 82, 313–318.
Jain, A.K., Singh., S. and Manickavasagam, R.M., 2002. Himalayan Collision Tectonics. Gondwana Research Group Memoir, 7, 114 p.
Jamieson, R.A., Beaumont, C., Medvedev, S. and Nguyen, M.H., 2004. Crustal channel flows: 2. Numerical models with implications for metamorphism in the Himalayan-Tibetan orogen. Journal of Geophysical Research, 109, B06407, 24 pp. doi: 10.1029/2003JB002811.
Jessup, M.J., Cottle, J.M., Searle, M.P., 2008. P-T-t-D paths of Everest Series schist, Nepal. Journal of Metamorphic Geology, 26, 717–739.
Kellett, D.A., Grujic, D., Warren, C., Cottle, J., Jamieson, R. and Tenzin, T., 2010. Metamorphic history of a syn-convergent orogen-parallel detachment: The South Tibetan detachment system, Bhutan Himalaya. Journal of Metamorphic Geology,28, doi:10.1111/j.1525-1314.2010.00893.x
Kohn, M.J., 2008. P–T–t data from Nepal support critical taper and repudiate large channel flow of the Greater Himalayan Sequence. Geological Society of America Bulletin, 120, 259–273.
Kohn, M.J., Wielnand, M., Parkinson, C.D., Upreti, B.N., 2005. Five generation of monazite in Langtang gneisses: implication for chronology of the Himalayan metamorphic core. Journal of Metamorphic Geology, 23, 399–406.
Langille, J., Lee, J., Hacker, B. and. Seward, G., 2010. Middle crustal ductile deformation patterns in southern Tibet: Insights from vorticity studies in Mabja Dome. Journal of Structural Geology, 32, 70–85.
Le Fort, P., 1975. Himalaya: the collided range. American Journal of Science, 275, 1–44.
Leloup, P. H., Mahéo, G. , Arnaud, N., Kali, E., Boutonnet, E., Liu, Dunyi., Xiaohan , Liu., and Haibing, Li, 2010. The South Tibet detachment shear zone in the Dinggye area. Time constraints on extrusion models of the Himalayas. Earth and Planetary Science Letters, 292, 1–16.
Montomoli, C., Iaccarino, S., Carosi, R., Langone, A., Visona, D., 2013. Tectonometamorphic discontinuities within the Greater Himalayan Sequence in Western Nepal (Central Himalaya): insights on the exhumation of crystalline rocks. Tectonophysics, 608, 1349–1370.

Passchier, C.W. and Trouw, R.A.J., 2005. Microtectonics. Springer, Berlin, 366 p.

Patel, R.C., Singh, S., Asokan, A., Manickavasagam, R.M. and Jain, A.K., 1993. Extensional tectonics in the Himalayan orogen, Zanskar. NW India. In Himalayan Tectonics (eds. Treolar, P.J. and Searle, M.P.), Geological Society, London, Special Publications, 74, p. 445–459.

Pêcher, A., 1989. The metamorphism in the Central Himalaya: Journal of Metamorphic Geology, 7, 31–41.

Sachan, H.K., Kohn, J.M., Saxena A. and Corrie, S.L., 2010. The Malari leucogranite, Garhwal Himalaya, Northern India: Chemistry, age and tectonic implications. Earth and Planetary Science Letters, 122 (11/12), 1865–1876.

Searle, M.P., 2010. Low-angle normal faults in the compressional Himalayan orogen; Evidence from the Annapurna–Dhaulagiri Himalaya, Nepal. Lithosphere, 6(4), 296-315.

Searle, M.P. and Godin, L., 2003. The South Tibetan Detachment System and the Manaslu Leucogranite: a structural reinterpretation and restoration of the Annapurna–Manaslu Himalaya, Nepal. Journal of Geology, 111, 505-523.

Searle, M.P., Windley, B.F., Coward, M.P., Cooper, D.J.W., Rex, A.J., Rex, D., Tingdong, L., Xuchang, X., Jan, M.Q., Thakur, V.C. and Kumar, S., 1987. The closing of Tethys and the tectonics of the Himalaya. Geological Society of America Bulletin, 98, 678–701.

Searle, M.P., Law R.D. and Jessup, M.J., 2006. Crustal structure, restoration and evolution of the Greater Himalaya in Nepal-South Tibet; implications for channel flow and ductile extrusion of the middle crust. In Law, R.D., Searle, M.P. and Godin, L. (eds) Channel Flow, Ductile Extrusion and Exhumation in Continental Collision Zones. Geological Society, London, Special Publications, 268, 355–78.

Searle M.P., Law R.D., Godin L., Larson K.P., Streule M.J., Cottle J.M. and Jessup, M.J., 2008. Defining the Himalayan Main Central Thrust in Nepal. Journal of Geological Society of London, 165, 523–534.

Spencer, C.J., Harris, R.A. and Dorais, M.J., 2012. The metamorphism and exhumation of the Himalayan metamorphic core, eastern Garhwal region, India. Tectonics, 31, TC1007, doi:10.1029/2010TC002853.

Stipp, M., Stunitz, H., Heilbronner, R. and Schmid S.M., 2002a. The eastern Tonale fault zone: A 'natural laboratory' for crystal plastic deformation over a temperature range from 250 to 700 °C. Journal of Structural Geology, 24, 1861–1884.

Stipp, M., Stünitz, H., Heilbronner, R. and Schmid, S., 2002b, Dynamic recrystallization of quartz: correlation between natural and experimental conditions. In: De Meer, S., Drury, M.R., De Bresser, J.H.P., Pennock, G.M. (eds.), Deformation Mechanisms, Rheology and Tectonics: Current Status and Future Perspectives. Geological Society, London, Special Publications, 200, 171–190.

ten Grotenhuis, S.M. , Trouw, R.A.J. and Passchier, C.W., 2003. Evolution of mica fish in mylonitic rocks. Tectonophysics, 372, 1–21.

Valdiya, K.S. and Pande, K., 2009. Behaviour of basement-cover decoupling in compressional deformation regime, northern Kumaun (Uttarakhand) Himalaya. Proceedings of the Indian National Science Academy, 75(1), 27–40.

Valdiya, K.S., 1980. Geology of the Kumaun Lesser Himalaya. Wadia Institute of Himalayan Geology, Dehra Dun, India., 249p.

Valdiya, K.S.,2005. Trans-Himadri fault: Tectonics of a Detachment System in Central Sector of Himalaya, India. Journal of Geological Society of India, 65, 537–552.

Valdiya, K.S., 1989. Trans-Himadri intracrustal fault and basement upwarps south of Indus-Tsangpo Suture Zone. In Tectonics of Western Himalaya (eds. Malinconico, L.L. and Lillie, R.J.). Geological Society of America (Special Papers), 232, 153–168.

Valdiya, K.S., Paul, S.K., Tarachandra, Bhakuni, S.S. and Upadhyay, R.C., 1999. Tectonic and lithological characterization of Himadri (Great Himalaya) between Kali and Yamuna rivers, Central Himalaya. Himalayan Geology, 10(2), 1-17.

Virdi, N.S., 1986. Lithostratigraphy and structure of the Central Crystallines in the Alaknanda and Dhauliganga valleys of Garhwal. In Himalayan Thrust and Associated Rocks (ed Saklani, P. S.), Today and Tomorrow's Printers & Publ., New Delhi, 10, 155–166.

Vannay, J.-C., and Hodges, K. V., 1996. Tectonothermal evolution of the Himalayan metamorphic core between the Annapurna and Dhaulagiri, central Nepal: Journal of Metamorphic Geology, v. 14, p. 635–656.

Waters, D.J., 2001. The significance of prograde and retrograde quartz-bearing intergrowth microstructures in partially melted granulite-faci-

es rocks. Lithos, 56, 97-110.
Webb, A.A.G., Yin, A., Harrison, T.M., Célérier, J. and Burgess, W.P., 2007. The leading edge of the Greater Himalayan Crystallines revealed in the NW Indian Himalaya: Implications for the evolution of the Himalayan Orogen. Geology, 35, 955–958, doi:10.1130/G23931A.1.
Wiedenbeck, M., Goswami, J.N. and Virdi, N. S., 2014. Singe zircon ^{207}Pb / ^{206}Pb ages from the Garhwal Himalaya (India): Paleo-Proterozoic magmatic activity in the Lesser and Higher Himalaya. Himalayan Geology, 35, 16–21.
Whitney, D.L., and Evans, B.W., 2010. Abbreviations for names of rock-forming minerals. American Mineralogist, 95, 185-187.
Yin, A., 2006. Cenozoic tectonic evolution of the Himalayan orogen as constrained by along-strike variation of structural geometry, exhumation history, and foreland sedimentation. Earth-Science Reviews, 76, 1–131.
Zhu, B., Kidd, W.S., Rowley, D.B., Currie, B.S. and Shafique, N., 2005. Age of initiation of the India-Asia collision in the east-central Himalaya. The Journal of Geology, 113, 265-285.